



PROCUREMENT EXECUTIVE, MINISTRY OF DEFENCE

Aeronautical Research Council  
Reports and Memoranda

THE USE OF SOUND ABSORBING WALLS  
TO REDUCE DYNAMIC INTERFERENCE  
IN WIND TUNNELS

by

D.G. Mabey  
Structures Department, RAE Bedford

LIBRARY  
ROYAL AIRCRAFT ESTABLISHMENT  
BEDFORD

London: Her Majesty's Stationery Office

£7 NET

UDC 533.6.071.11 : 534.833.532 : 533.6.071.4 : 534.242

THE USE OF SOUND ABSORBING WALLS TO REDUCE DYNAMIC INTERFERENCE  
IN WIND TUNNELS

By D. G. Mabey

Structures Department, RAE Bedford

---

REPORTS AND MEMORANDA NO.3831\*

November 1976

---

SUMMARY

A scheme for reducing dynamic interference in wind tunnels at subsonic and transonic speeds was tested in a pilot 4in × 4in tunnel. Two types of dynamic interference were considered: excitation of unwanted acoustic resonances within the working section and flow unsteadiness. The tests show that both types of interference could be substantially reduced by replacing the conventional hard walls of a closed or a slotted working section by appropriate sound absorbing walls.

The models used to establish the resonances in the working sections with hard walls were small circular cylinders operating in the subcritical Reynolds number range  $(R_d < 2 \times 10^5)$  and thus generating discrete pressure fluctuations at the vortex shedding frequency. When the resonances were suppressed by the wall material the pressure fluctuations agreed well with previous measurements made in a much larger, low speed wind tunnel, and with predictions.

The results of this small scale test were judged sufficiently encouraging to justify a further investigation in the RAE 3ft × 3ft tunnel, which it is hoped will include tests of an oscillating model.

---

\* Replaces RAE Technical Report 76157 - ARC 37436

CONTENTS

	<u>Page</u>
1 INTRODUCTION	3
2 DESIGN OF EXPERIMENT	4
2.1 Choice of model	4
2.2 Choice of working sections	5
3 EXPERIMENTAL DETAILS	6
3.1 Circular cylinders and test conditions	6
3.2 Working sections	8
3.3 Pressure transducers and instrumentation	10
4 RESULTS	11
4.1 Pressure fluctuations induced by vortex shedding from circular cylinders	12
4.1.1 Closed working sections	12
4.1.2 Slotted working sections	16
4.1.3 Perforated working section	19
4.2 Flow unsteadiness in empty working sections	21
4.2.1 Closed working sections	21
4.2.2 Slotted working sections	23
4.2.3 Perforated working section	26
5 DISCUSSION	27
6 CONCLUSIONS	31
Acknowledgments	32
Appendix Properties of wall materials	33
Symbols	36
References	37
Illustrations	Figures 1-30
Detachable abstract cards	-

## 1 INTRODUCTION

There is currently great interest in increasing the Reynolds number range available for tests on wind tunnel models at transonic speeds. One way to increase the Reynolds number without additional expense is to ensure that the largest possible model\* can be tested in a working section of any given size, without degrading the accuracy of the measurements.

This challenge led Sears to suggest the concept of "the self-correcting wind tunnel"<sup>1</sup>. In this tunnel the boundary conditions on a control surface within the working section (generally adjacent to the tunnel walls) would be measured for the steady flow about the model and then adjusted, by altering the tunnel walls, until the measured boundary conditions agree with those calculated at corresponding points in the unbounded flow for the forces measured on the model. Thus, at the end of an iterative process, which should be convergent, the wall interference corrections for steady flow would be identically zero and the forces and moments measured on the model would be correct for that Reynolds number. Initial tests of the concept are promising and it is possible that new transonic facilities will be provided with some form of 'self-correcting walls'.

The present research stems from the thought that these 'self-correcting walls' might also incorporate features which would reduce the dynamic interference effects which occur in wind tunnels. This Report describes how dynamic interference has been reduced in a preliminary experiment in a small wind tunnel and suggests how the method could be applied in a larger facility.

The dynamic interference effects we wish to eliminate are resonances and flow unsteadiness caused by the tunnel walls. Both of these effects may be important during tests of models for the prediction of flutter boundaries or the severity of buffeting, and both might be alleviated by the use of sound absorbing material for the walls.

It has been suggested that tunnel resonance can vitiate flutter measurements on swept wing models at high subsonic and transonic speeds<sup>2</sup> and that tunnel noise determines the length of time required to make accurate subcritical damping measurements<sup>3</sup>. The latter consideration suggests that levels of flow unsteadiness previously regarded as acceptable for flutter tests in continuous facilities<sup>4</sup> would be unacceptable in intermittent facilities<sup>5</sup>.

---

\* When large models are used for aeroelastic tests it is much easier to scale spars and skin thicknesses.

There is also a possibility that buffeting measurements at transonic speeds are influenced by dynamic wall interference, for strong pressure waves are generated by the separated flows which excite buffeting and these pressure waves could be reflected back onto the model, unless special walls are used to absorb them. Naumann showed pressure waves propagating away from a circular cylinder at subsonic speeds, and their reflections by hard walls<sup>6</sup>. He also showed that the strength of the reflections could be substantially reduced if the walls were lined with sound absorbing materials. (The high-speed cine films taken with a schlieren system should be carefully compared in Figs.25 and 26 of Ref.6.) His experiment was the starting point for these tests.

A quick survey of this paper may be obtained by reading sections 2, 5 and 6.

## 2 DESIGN OF EXPERIMENT

### 2.1 Choice of model

The ideal choice for this type of experiment would be the measurement of fluctuating pressures at transonic speeds on an oscillating model in a small wind tunnel. The fluctuating pressures on this model could then be measured for different wall materials and compared with an 'interference-free' datum provided by measurements on the same model in a much larger transonic tunnel at the same Reynolds number. It is hoped that this ideal test may yet be completed. However, the only wind tunnel available for these preliminary tests was small (with a working section of 10mm × 10mm). A model for this working section, with a chord of only 25mm and incorporating pressure transducers, would have been difficult to construct. In addition the tunnel total pressure is only about 1 bar, so that with a model of this chord the largest test Reynolds number would only be  $0.4 \times 10^6$  at transonic speeds. A Reynolds number as low as this would invite serious criticism of the experiment, even with fixed transition on the model. Hence an alternative, less direct method was adopted.

An easily reproducible, two-dimensional shape was sought which would produce a strongly oscillatory flow with known properties over an appropriate range of Reynolds number. Modifications to the wall material and the wall geometry would then modify the oscillatory flow on the model if significant dynamic interference occurred.

The models selected were small circular cylinders operating at subcritical Reynolds numbers. For the subcritical range ( $10^3 < R_d < 2 \times 10^5$ ), an isolated circular cylinder of diameter  $d$  in an unbounded free stream of velocity  $u$

sheds vortices at a discrete frequency,  $f^*$ , given by the relation:

$$f^* = S^*u/d, \quad (1)$$

where  $S^*$  = dimensionless shedding frequency or Strouhal number (about 0.21 within the subcritical Reynolds number range). Equation (1) is well documented for an unbounded stream so that serious deviations from it could be directly attributed to wall interference.

The strongly oscillatory flow about the circular cylinder generates a large fluctuating lift coefficient (the measurements are rather difficult but the levels vary from about  $\bar{C}_L = 0.4$  to 0.7 rms at the shedding frequency  $f^*$ ) and a smaller fluctuating drag coefficient (about  $\bar{C}_D = 0.1$  rms at a frequency  $2f^*$ ). The oscillatory flow generates pressure waves which propagate away from the model and then are reflected by the tunnel walls. This reflection process is similar to that which introduces interference effects in dynamic tests, such as flutter or buffeting measurements.

The level of the fluctuating forces acting on a circular cylinder is so large that the forces are more akin to those found on an aircraft model under conditions of heavy buffeting at transonic speeds\* rather than those caused by the usual small amplitude oscillation of a wing or of a trailing-edge control. For our purpose here these large fluctuating forces are advantageous because they ensure that dynamic wall constraint effects are easily noticed and measured.

An advantage of restricting the preliminary tests to the Mach number range from  $M = 0.3$  to 0.6 is that the flow unsteadiness then generally remains roughly constant. In contrast, above  $M = 0.6$  the flow unsteadiness generally increases rapidly until it reaches a maximum at about  $M = 0.8$  and then decreases.

## 2.2 Choice of working sections

A previous investigation<sup>4</sup> suggested that the small wind tunnel available (the RAE pilot 4in x 4in tunnel, a 1/9-scale model of the RAE 3ft x 3ft tunnel) gives good indications of the flow unsteadiness in the full-scale tunnel with closed and slotted working sections. Hence the emphasis in the present comparative tests was on closed and slotted working sections of different wall materials. These wall materials were incorporated in alternative top and bottom liners

---

\* The buffet excitation on an aircraft at transonic speeds generally extends over a wide range of frequencies.

(Fig.1). The side walls of the working section were hard and remained unchanged during the experiment; they were instrumented with seven pressure transducers.

Perforated walls with  $60^\circ$  inclined holes are used in some transonic tunnels and limited tests were made with top and bottom walls of this type with open area ratio 6% (3% overall). In a small tunnel of this size it would not be easy to incorporate sound absorbing material into perforated liners. Hence no variation in wall material was attempted.

### 3 EXPERIMENTAL DETAILS

#### 3.1 Circular cylinders and test conditions

Two solid steel cylinders with diameters of 10 and 18mm were used. The surface finish varied between 0.4 to  $1.1\mu\text{m}$  rms but this should not affect vortex shedding in the subcritical Reynolds number range<sup>7</sup>. The cylinder diameters were selected to achieve a coincidence between the vortex shedding frequency,  $f^*$ , and the predicted<sup>8</sup> two-dimensional tunnel resonance frequency for transverse waves,  $f_r$ , at a design Mach number of about  $M = 0.4$  in the closed and slotted working sections, as Fig.2 and the following table show.

Cylinder d(mm)	Predicted	Design	Figure
	resonance frequency $f_r$ (Hz)	Mach number M	
18	1500 closed	0.39	2a
10	2600 slotted	0.39	2b

The cylinders were directly mounted in inserts (Fig.1) slid into the tunnel sidewalls, so that no gaps occurred at the ends of the cylinders which would have influenced the measurements.

The blockage of the cylinders was so high as to magnify both the static and dynamic interference effects. The choking Mach numbers for the cylinders in the closed working section calculated by one-dimensional theory agreed roughly with the measured values, as the following table shows.

Cylinder d(mm)	Blockage (%)	Choking Mach number	
		Calculated	Measured
18	18	0.55	0.53
10	10	0.66	0.62

The high blockage ratios of the cylinders made the choice of a reference Mach number rather difficult. Static pressure measurements along the centre line of the sidewall of the closed working sections (at the same streamwise distances,  $x$ , as the first five pressure transducers, Fig.1) showed that the cylinders induced significant upstream adverse pressure gradients as compared with the tunnel empty distribution (Fig.3). Similar trends were shown both by the wall static and the plenum chamber pressures for the slotted and perforated working sections (Figs.4 and 5). For the slotted working sections it was noticed that the middle plenum chamber pressure, at  $x/H = 2.0$ , was almost the same as the sidewall pressure at  $x/H = 1.5$ , both with the tunnel empty and with the 18mm diameter cylinder. Hence the following reference static pressure locations were somewhat arbitrarily adopted:

- Closed working section (sidewall)  $x/H = 1.5$
- Slotted working section (plenum)  $x/H = 2.0$  (scaled centre of rotation for models in RAE 3ft tunnel)
- Perforated working section (plenum)  $x/H = 2.0$  (scaled centre of rotation for models in RAE 3ft tunnel).

The unresolved uncertainties in the absolute Mach numbers cannot affect the validity of comparisons made for a particular cylinder between geometrically identical working sections made of different materials as long as the corresponding average Mach number distributions are identical. However, these uncertainties could have a minor influence on the comparisons made between working sections of different types (say between the closed and perforated working sections). The differences in true Mach number at the cylinder undoubtedly account for some of the variation in the measured Strouhal numbers shown in the subsequent figures.

The total pressure and total temperature of the RAE 4in  $\times$  4in tunnel cannot be independently controlled, and this leads to a further uncertainty in the precise test Reynolds numbers. (This is an additional reason for selecting models with a flow relatively insensitive to variations in Reynolds number in the range of interest.) In the mode of operation used in these tests ('closed circuit exhaust') the tunnel total pressure is always a little lower than the ambient atmospheric static pressure and the total temperature lies in the range from about 10°C to 15°C. The actual test Reynolds numbers are always within about  $\pm 3\%$  of the mean values quoted and remain in the subcritical range ( $10^3 < R_d < 2.10^5$ ) for which vortex shedding occurs.



### 3.2 Working sections

Fig.1 shows the general arrangement of the circular cylinders in the perspex transonic working section. The cylinders were placed at  $x/H = 2.5$  ,  $0.5H$  downstream of the usual model centre of rotation at  $x/H = 2.0$  . This position facilitated the study of the pressure waves moving upstream into the undisturbed flow, observed in Naumann's experiment<sup>6</sup>.

Seven small pressure transducers were flush-mounted in one tunnel sidewall at streamwise intervals of  $0.5H$ . These transducers were displaced  $0.25H$  below the tunnel centre line to allow the measurement of pressure fluctuations adjacent to the cylinders and to ensure that the fundamental transverse tunnel resonance could be detected. (This has an anti-node on the tunnel centre line and a node at the wall which gives zero pressure fluctuations on the centre line and a maximum at the wall.)

In addition to the local pressure fluctuations in the free stream every pressure transducer received high frequency excitation (in the range from 10 to 100kHz) from the thin sidewall boundary layers. However this excitation was above the flat frequency response range of the instrumentation (given as 6kHz in section 3.3), and thus was not measured. The excitation would be constant for a particular transducer at a given Mach number and Reynolds number because no changes were made in the tunnel sidewalls throughout the experiment. For reference purposes, this unmeasured rms broadband tare correction<sup>9</sup> for an attached turbulent boundary layer in zero pressure gradient is estimated to be

$$\bar{p}/q = 2.5C_f \quad (2)$$

where  $q$  = kinetic pressure,

and  $C_f$  = local skin friction coefficient.

Modifications to the tunnel working section were made by withdrawing the liner sidewall extension and fitting alternative top and bottom liners. The liner/sidewall extension shown in Fig.1 maintains the 4in  $\times$  4in working section for an additional length of one tunnel height for operation of the closed working sections. An alternative sidewall extension was provided for operation of the slotted and perforated working sections. This extension starts with a sudden expansion to a constant 114mm  $\times$  114mm section which thus creates adequate diffuser suction for transonic operation.

Closed and slotted liners were made from three different materials, namely:-

- (1) Wood or perspex to represent conventional tunnel liners with hard walls.
- (2) Low density sound absorbing foam covered by a perforated PVC laminate.
- (3) Low density sound absorbing foam.

For brevity, most of the tests reported here are restricted to the first two materials, although all three materials were tested. Throughout the Report these materials are described as

hard,  
laminate and  
foam.

Some information on the physical and acoustic properties of the laminate and foam materials is given in the Appendix. The laminate had a good aerodynamic finish whereas the foam had a comparatively rough surface which appeared likely to cause additional boundary layer growth.

Fig.6 (which is not drawn to scale) shows the main features of the slotted liners, which have an open area ratio of 17% on the top and bottom walls, giving a ratio of 8.5% based on all four walls. The slots have a straight taper for the initial expansion of the flow over a streamwise length of  $0.5H$ ; for the remainder of their length the slots have a constant width of  $0.034H$ . This simple geometry was adopted to ease the problems of constructing such small working sections with the laminate and foam materials, but it produces relatively poor Mach number distributions in the working section at transonic speeds. (A working section for a larger tunnel would incorporate the standard slot shape developed by the NACA<sup>10</sup> which provides a good Mach number distribution.)

Fig.6 also shows that the slats are excessively deep by normal standards for transonic tunnels, because a significant thickness of laminate or foam (13mm) is required to develop a useful attenuation at the frequencies of interest (1 to 5kHz). The thickness of laminate or foam used in the closed working section was 25mm, so that the sound absorbing properties of the closed walls were different from those of the slats in the slotted working section at the frequencies of interest (Appendix).

Venting holes in the I beams supporting every slat equalise the lateral variation of plenum chamber pressures. The top and bottom plenum chambers are connected to the side plenum chambers via venting holes passing through each of

the sidewalls, which are within the perspex shell. Thus the ratio of plenum chamber volume/working section volume,  $V_p/V_w$ , is increased to about 0.80. Although this value is low, it is higher than that currently used in the top and bottom slotted section of the RAE 3ft x 3ft tunnel ( $V_p/V_w = 0.30$ ). The ratio provided should be adequate to eliminate excessive pressure gradients in the plenum chamber with models of normal blockage (1 to 2%).

Figs.3 to 5 show that there is a small favourable pressure gradient at the start of all the working sections at the first streamwise pressure transducer ( $x/H = 0$ ).

### 3.3 Pressure transducers and instrumentation

The pressure transducers used for this experiment were of the semi-conductor strain gauge type, having a diaphragm of 3.2mm diameter. They were connected to ac coupled amplifiers having a gain of about 900/1. The gain of every amplifier was adjusted so that the sensitivity of all the transducers was identical -  $3.29\text{kN/m}^2/\text{V}$  (0.97in Hg/V). The dynamic calibration of all the transducers was made with a pistonphone at a single frequency of 50Hz, but the combined response of the transducers and amplifiers should be flat over the range from dc to about 6kHz.

The voltages from the transducers were manually monitored on a Brüel and Kjaër spectrum analyser Type 2107, which was used primarily as a tuneable filter. The recorder output from the analyser was used either to generate spectra using a Brüel and Kjaër level recorder, Type 2305, or to display the broadband signal or narrow bandwidth tuned signal on a DISA rms voltmeter, Type 55D 35. The time constant of this meter could be adjusted to ensure steady readings. (Normally a 1 second time constant was adequate.)

In this Report the sidewall pressure fluctuation measurements are plotted in three non-dimensional forms. Most of the measurements are of the level of pressure fluctuations generated by the circular cylinder at the vortex shedding frequency,  $f^*$  (section 4.1). Hence these measurements are plotted in terms of the root mean square (rms) pressure fluctuation coefficient,  $\bar{p}/q$ , within a narrow bandwidth

$$\Delta f = \epsilon f, \tag{3}$$

where  $\epsilon$  = the analyser bandwidth ratio.

For consistency the same narrow bandwidth

$$\epsilon = 0.06$$

was used throughout the tests.

For the smaller number of measurements made with the tunnel empty (section 4.2) the pressure fluctuation spectra are continuous. Although broad peaks occur at particular frequencies these measurements are best expressed in terms of either the broadband rms pressure coefficient  $\bar{P}/q$ , or the level of flow unsteadiness for a continuous spectrum:

$$\sqrt{nF(n)} = \bar{p}/q(\epsilon)^{\frac{1}{2}} . \tag{4}$$

The definition of  $\sqrt{nF(n)}$  is derived from the mean square pressure fluctuation coefficient

$$\bar{P}^2/q^2 = \int_0^{\infty} F(n)dn , \tag{5}$$

where  $n = fw/u$  is conventionally based on the tunnel width,  $w$ , and where  $F(n)dn$  is the contribution to the mean square pressure fluctuation coefficient in a small frequency parameter of bandwidth  $dn$ .

It should be emphasised again that the main objective of these tests is the comparison (at particular points on the sidewall) of the pressure fluctuations generated by the cylinders for different top and bottom walls. Hence the absolute level of the measured pressure fluctuations is not essential. Thus there is no need to discuss possible effects of transducer cavity resonance, the surface finish and pressure loss/volume flow characteristics of the transducer orifices or of the variation of the sidewall boundary layer along the working section; moreover, these effects are believed to be small.

#### 4 RESULTS

In this experiment the dynamic interference effects in the different working sections can be conveniently considered under the separate headings of the variations in the pressure fluctuations induced by vortex shedding from the circular cylinders (section 4.1) and of the flow unsteadiness in the empty working sections (section 4.2). The variations in acoustic resonances and

reflected pressure waves in the different working sections have first order effects on the measured pressure fluctuations induced by vortex shedding, whereas the corresponding, simultaneous variations in flow unsteadiness in the different working sections have relatively minor or second order effects on the vortex shedding (section 4.2.2).

4.1 Pressure fluctuations induced by vortex shedding from circular cylinders

4.1.1 Closed working sections

Measurements are given with the alternative hard and laminate walls forming the top and bottom of the working sections.

Fig.7 shows the non-dimensional narrow bandwidth pressure fluctuations,  $\bar{p}/q$ , induced by the 18mm diameter cylinder in the closed working sections. As the tunnel speed is varied, we find for the design condition of the experiment at  $M = 0.4$  (Fig.2a and section 3.1) a severe resonance with hard walls. Here the vortex shedding frequency

$$f^* = 1530 \text{ Hz ,}$$

is close to the calculated transverse resonance frequency for a two-dimensional working section

$$f_r = 1490 \text{ Hz .}$$

Fig.7 also shows that with hard walls the pressure fluctuations adjacent to the cylinder at  $x/H = 2.5$  become extremely large†, and vary widely (from  $p/q = 40\%$  to  $80\%$ ) from day to day.

The streamwise variation of the pressure fluctuations is interesting and is now considered in some detail because similar variations occur in subsequent tests. The pressure fluctuations first decrease moving upstream and then increase to reach a maximum between  $x/H = 0.5$  and  $x/h = 1.0$ . Now for an infinitely long two-dimensional duct, the frequency of the transverse resonance excited by the cylinder would correspond with the so-called 'cut off frequency'. (The propagation of sound in infinitely long ducts with and without flow is discussed in Ref.11.) Below this 'cut-off frequency' the amplitude of the longitudinal

---

† The external noise level outside the tunnel also became excessive as this resonance condition was approached, and was clearly observed in the room above the tunnel.

pressure fluctuations would decay exponentially away from the cylinder. However, at or above the 'cut-off' frequency the pressure fluctuations could propagate to infinity along the duct as waves of constant strength. In ducts of finite length, as in the present experiment, the precise computation of the duct modes is much more difficult<sup>12,13</sup>. Some of these difficulties are analytical, others arise because of the uncertainty about the physical boundary conditions appropriate to the ends of the duct. However, at or above the 'cut-off' frequency the pressure fluctuations can still propagate significant distances along the duct so that the wave form shown in Fig.7 with hard walls is not surprising, even though the precise wave form may not yet be calculable.

In marked contrast to these results for the hard wall, with the laminate walls there is no obvious resonance. The pressure fluctuations adjacent to the cylinder are only about  $\bar{p}/q = 20\%$  and the pressure fluctuations attenuate monotonically moving upstream so that there is no streamwise mode. Thus for this condition the closed working section with hard walls gives grossly inaccurate measurements relative to the unconstrained flow.

We see a rather different situation at the lower Mach number,  $M = 0.3$ , when the vortex shedding frequency should be less than the transverse resonance frequency (Fig.2a). With the hard walls the cylinder induces lower pressure fluctuations than at  $M = 0.40$ , but at two discrete frequencies. The first frequency is

$$f^* = 1300 \quad \text{Hz}$$

which corresponds with  $S^* = 0.24$ . This is somewhat higher than the standard Strouhal number,  $S^* = 0.21$ . The second frequency is

$$f^* = 1600 \quad \text{Hz}$$

which corresponds with  $S^* = 0.29$ . This frequency is probably forced by the transverse resonance, shown in Fig.2a to be

$$f_r = 1550 \quad \text{Hz}$$

and the pressure fluctuations persist undiminished at a high level ( $\bar{p}/q \geq 7\%$ )

upstream to  $x/H = 1.0$  . This plainly represents a serious interference effect. In contrast the laminate walls eliminate this spurious mode and reduce the pressure fluctuations caused by the first mode. Again the closed working section with hard walls manifestly gives inaccurate measurements relative to the unconstrained flow.

We see that at the highest Mach number,  $M = 0.5$  , the pressure fluctuations with the hard walls are considerably lower than they are at  $M = 0.4$  . This should probably be attributed to a reduction in the excitation caused by vortex-shedding as the flow approaches the choking condition ( $M_c = 0.53$ ). Fig.2a shows that no resonance was predicted at this speed, for the vortex shedding frequency is above the tunnel transverse resonance frequency. However the streamwise mode persists, the pressure fluctuations first decreasing in the upstream direction and then increasing to reach a maximum again giving a streamwise distance  $1.8H$  (nearly the transverse wavelength) between the maxima at about  $x/H = 0.5$  and  $x/H = 2.3$  . In contrast, with the laminate walls the level of pressure fluctuations is considerably lower and the pressure fluctuations measurements attenuate monotonically in the upstream direction.

The measurements in Fig.7 suggest that in a closed working section with hard walls, any phenomenon in which a vortex shedding frequency approaches or coincides with a transverse resonance frequency could be subject to serious interference effects. If interference of this type occurs, the vortex shedding could be altered and no simple corrections could be applicable to the measurements. The laminate walls plainly offer an effective means of drastically reducing such interference effects in a closed working section.

Fig.8 shows the narrow bandwidth pressure fluctuations,  $\bar{p}/q$  , induced by the 10mm diameter cylinder in the closed working section with hard and laminate walls. There is a severe resonance with the hard walls at  $M = 0.24$  , when the vortex shedding frequency (see Fig.2a),

$$f^* = 1650 \quad \text{Hz}$$

corresponds roughly to the predicted transverse resonance frequency

$$f_r = 1580 \quad \text{Hz} .$$

The pressure fluctuation coefficients measured are large (although the measurements are not very accurate because of the small kinetic pressure), about  $\bar{p}/q = 49\%$  adjacent to the cylinder. In addition the streamwise mode is excited,

with large pressure fluctuations upstream of the cylinder. In contrast to the measurements with the hard walls, with the laminate walls there is no obvious resonance. The situation is generally similar in character to that for the 18mm diameter cylinder at its resonance condition according to Fig.2a (i.e.  $M = 0.4$  in Fig.7).

With the 10mm diameter cylinder, for Mach numbers above  $M = 0.24$ , Fig.2a shows the vortex shedding frequency is higher than the predicted transverse resonance frequency and hence no other transverse resonance should occur. However within the working section with hard walls there is a streamwise mode at the vortex shedding frequency (above the 'cut-off frequency') which the laminate wall suppresses. Hence the laminate walls would also be preferred for tests of this small cylinder in the closed working section.

A brief comparative evaluation of the effectiveness of the laminate and foam walls in suppressing the spurious pressure fluctuations was also made. Fig.9 shows that both the foam and laminate walls eliminate the resonances discussed above for the 18mm diameter cylinder. However the foam walls were judged slightly inferior to the laminate walls from  $M = 0.3$  to  $0.4$  (i.e. from  $f^* = 1200$  to  $1700\text{Hz}$ ) because the pressure fluctuations measured were a little higher. This is probably related with the higher sound-absorption coefficients of the laminate walls measured in this range of frequency (see discussion of Fig.30 in the Appendix). The results for  $M = 0.5$  show the same trend but must be less convincing because they are so close to choking at  $M = 0.52$ .

Fig.10 shows similar measurements for the 10mm cylinder, but here the foam walls were slightly superior to the laminate walls from  $M = 0.3$  to  $0.4$  (i.e. from  $f^* = 2000$  to  $2650\text{Hz}$ ). In this frequency range the sound-absorption coefficients for laminate and foam walls have much the same value. The results for  $M = 0.5$  are inconclusive because the measured level of pressure fluctuations is so small with both walls.

It is interesting to note that transverse resonances in closed working sections can be significantly attenuated even by a single wall formed by sound absorbing material (Fig.11). Thus with the 10mm diameter cylinder at  $M = 0.24$  the strong resonance observed with two hard walls is almost equally well suppressed by either a laminate top wall and a hard bottom wall, or by two laminate walls. With the 18mm diameter cylinder at the design condition at  $M = 0.4$  the strong resonance obtained with two hard walls is more difficult to suppress. However, the replacement of the top hard wall by a laminate wall



makes a great improvement, though admittedly not as great as with two laminate walls. These asymmetric wall configurations could be useful in low speed tunnels. Here the floor of the working sections must generally be hard to permit rigging of models. In contrast the roof of the working section is often made of wood and could be replaced with sound absorbing laminate without too much difficulty.

#### 4.1.2 Slotted working sections

Measurements are given with the slats made of the alternative hard and laminate materials, for both of which the depth of material is limited to 13mm to ensure an adequate plenum chamber volume (see section 3.2 above).

Fig.12 shows the narrow bandwidth pressure fluctuations,  $\bar{p}/q$ , induced by the 10mm diameter cylinder in the slotted working sections.

For the design condition of this cylinder at  $M = 0.4$  (Fig.26 and section 3.1), no resonance occurs with hard slats even though the measured vortex shedding frequency

$$f^* = 2700 \quad \text{Hz} ,$$

corresponds closely with the predicted<sup>8</sup> transverse two-dimensional resonance frequency

$$f_r = 2660 \quad \text{Hz} .$$

Hence either the slotted working section provides a strong natural attenuation of the resonance mode, (even with hard slats), or the transverse resonance frequency is different from the predicted value. In the author's view the evidence to be presented suggests that both these hypotheses are valid. Some uncertainty must be expected because of the different boundary conditions appropriate to the slats and the slots.

It is interesting to note that with the hard slats at  $M = 0.4$  there is a streamwise mode at the vortex shedding frequency, similar to that observed with hard walls in the closed working section (Fig.8) but much smaller. This suggests that the vortex shedding frequency is above the 'cut off frequency'. This streamwise variation is reduced by the laminate slats, but is still not completely eliminated. The same features are apparent at the lower Mach number,  $M = 0.3$ , but here the laminate walls completely eliminate the upstream variation of the pressure fluctuations, which may be tentatively attributed to a resonance.

The pressure fluctuations for the 10mm cylinder are small in both working sections at  $M = 0.5$ , consistent with the mismatch between  $f^*$  and  $f_r$  (Fig.2b) and the fact that the vortex shedding is much reduced by the development of transonic flow around the cylinder at this Reynolds number. These measurements again resemble those made on the same cylinder in the closed working section (Fig.8), with a small streamwise variation in the slotted working section with hard walls, which is eliminated by the laminate walls.

It was suspected that the transverse resonance frequency in this slotted section might be only a little higher than in the closed working section. Hence an attempt was made to confirm the resonance on the 10mm diameter cylinder close to  $M = 0.30$  (Fig.13). Fig.13a shows the broadband pressure fluctuations ( $\bar{P}/q$ ) close to the start ( $x/H = 0.5$ ) of the slotted working section with hard slats; there is a reasonably well defined maximum at  $M = 0.31$  consistent with a resonance condition (at least with respect to the streamwise variation). The narrow band pressure fluctuations for this speed for all the other transducers (Fig.13b), show no reduction from  $x/H = 1.5$  to 1.0, even though the Strouhal number was reasonable ( $S^* = 0.20$ ). The shedding frequency was

$$f^* = 2030 \quad \text{Hz}$$

and later evidence suggests that this is close to a transverse resonance frequency of about  $f_r = 2000\text{Hz}$ , somewhat higher than that in the closed tunnel at the same speed (1550Hz).

Fig.14 shows the pressure fluctuation measurements for the 18mm diameter cylinder, for which no transverse resonance is predicted in the range from  $0.3 < M < 0.5$  (Fig.2b). The level of pressure fluctuations is generally higher with the hard slats than with laminate slats. In addition the laminate slats reduce the streamwise variation both at  $M = 0.40$  ( $f^* = 1575\text{Hz}$ ) and at  $M = 0.50$  ( $f^* = 2000\text{Hz}$ ).

Comparison of Figs.14 and 7 shows that with the laminate walls the pressure fluctuations measured in both the slotted and closed working sections are in fair agreement at  $M = 0.3$  and 0.4. The apparent differences at  $M = 0.5$  may be attributed to the fact that this speed is close to the choking Mach number ( $M_c = 0.52$ ) in the closed working section.

An attempt was then made to establish if a 'resonance' could be excited by the 18mm cylinder in the slotted working section with hard slats. The broadband pressure fluctuations ( $\bar{P}/q$ ) close to the start of the working section (at

$x/H = 0.5$ ) were measured for small increments in Mach number close to  $M = 0.50$ . A reasonably well defined maximum was obtained at  $M = 0.51$  (Fig.15a), which suggests that this might be a 'resonance' condition close to a 'cut off' frequency, (*cf.* Fig.13a). However, this tentative conclusion should be viewed with caution. The cylinder is operating well above the critical Mach number and it is probable that the pressure fluctuations radiated forward of the cylinder in an unbounded stream might well have a maximum at about  $M = 0.51$ , even in the absence of a resonance condition.

This maximum must be expected because mutually opposing features occur in the flow. The magnitude of the pressure fluctuations generated at the terminal shock wave (which is unsteady) will increase rapidly as the transonic flow region develops around the cylinder. However, these pressure fluctuations will no longer be able to propagate directly upstream because of the sonic region, although they will be able to propagate round the boundaries of the sonic flow region. In addition the progressive expansion of the transonic flow region ultimately narrows and weakens the vortex wake, until at supersonic speeds no discrete vortex shedding occurs.

Despite this reservation, the corresponding streamwise narrow bandwidth pressure fluctuations (Fig.15b) have maxima at about  $x/H = 2.5$  and  $0.5$  and a minimum at  $x/H = 1.5$ . The Strouhal number was a little higher ( $S^* = 0.22$ ) than the usual value, but this is not significant in the light of the possible blockage correction.

What is more interesting is that the vortex shedding frequency from the 18mm cylinder at  $M = 0.51$  is

$$f^* = 2120 \quad \text{Hz (Fig.15b) ,}$$

and this is roughly the same as that found for the 10mm cylinder at  $M = 0.31$

$$f^* = 2030 \quad \text{Hz (Fig.13b) .}$$

Although it could be fortuitous, this rough coincidence suggests that the transverse resonance frequency in the slotted working section with hard walls and open area ratio 17% may be about 30% higher than with the fully closed hard walls at the same Mach number, rather than about 75% higher as predicted<sup>8</sup>. (The resonance frequency should fall with increasing Mach number.)

A further investigation of possible transverse resonances was attempted using the slotted working section with hard walls. All of the slots were sealed with sellotape to form a 'closed' 100mm × 100mm working section. With the 18mm cylinder, a Mach number of  $M = 0.4$  was established, using the sidewall reference static hole. A strong resonance occurred (Fig.16a), which corresponded fairly well in level and frequency with that observed previously in the closed working section with hard walls (Fig.7); this was certainly a transverse resonance condition.

The sellotape covering the central slot of the top and bottom liners was then removed, increasing the open area ratio from 0 to 4%. A significant reduction in pressure fluctuations throughout the working section was then observed, with virtually no change in frequency. This observation is certainly consistent with a large increase in acoustic damping with a comparatively small increase in open area ratio and a small variation in resonance frequency. The sellotape was then removed progressively from the adjacent slots, increasing the open area ratio to 12% and 20%, with corresponding reductions in pressure fluctuations and with comparatively minor changes in frequency. (These tests were made in an early part of the test programme when the fully open area ratio was 20%, not 17% as in the main series of tests.)

We may call the transducer positions adjacent to the cylinder ( $x/H = 2.5$ ) the near field and at  $x/H = 1.0$  the far field. Using the measurements at each point for zero open area ratio as reference values,

$$(\bar{P}/q)_0 ,$$

we may then plot the attenuation of the near field and far field measurements,

$$(\bar{P}/q)/(\bar{P}/q)_0 ,$$

as a function of open area ratio. Fig.16b suggests that quite small open area ratios (i.e. small amounts of ventilation) will strongly attenuate transverse acoustic resonance, even in a slotted working section with hard slots.

#### 4.1.3 Perforated working section

For the tests of a perforated working section with  $60^\circ$  inclined holes and 6% open area ratio only hard liners were used. These were not made specially for these tests, but were adapted from a previous investigation in the 4in × 4in tunnel (Ref.4, Figs.7 and 8).

Fig.17 suggests that for the 10mm cylinder there are no severe interference effects, although the pressure fluctuations upstream of the cylinder do not attenuate as they should at  $M = 0.4$ , suggesting that the vortex shedding frequency is above a 'cut-off' frequency. Apart from this, the pressure fluctuations correspond fairly well with those measured in the closed (Fig.8) and slotted (Fig.12) working sections with laminate walls. For the 18mm cylinder, Fig.18 suggests that there are no severe interference effects, the pressure fluctuations again corresponding broadly with those previously measured in the closed (Fig.7) and slotted (Fig.14) working sections with laminate walls. The low Strouhal number of both cylinders ( $S^* = 0.18$ ) reflects the uncertainty about the true Mach number at the cylinder and implies that the reference kinetic pressures,  $q$ , are in error (see discussion of Figs.4 and 5 in section 3.1).

An investigation of possible transverse resonances in the hard perforated working section was then made, following the method adopted for the hard slotted working section (see discussion of Fig.16). The perforated top and bottom walls were sealed with sellotape to form a 'closed' 100mm  $\times$  100mm working section. With the 18mm cylinder a Mach number of  $M = 0.4$  was established, using the sidewall reference static hole. A strong resonance occurred (Fig.19a), which corresponded fairly well in level and frequency with that observed previously in the closed working section with hard walls (Fig.7); this was certainly a transverse resonance condition.

The sellotape covering the middle  $\frac{1}{3}$  of the top and bottom walls was then removed, increasing the open area ratio from 0 to 2%. A significant reduction in pressure fluctuations throughout the working section was then observed, with virtually no change in frequency. Just as in the corresponding experiment in the hard slotted working section (Fig.16), Fig.19 suggests there is a large increase in acoustic damping with a comparatively small increase in open area ratio. There is also a small variation in vortex shedding and resonance frequencies. The sellotape was then removed progressively from the perforated walls, increasing the open area ratio to 4% and 6%, with corresponding reductions in pressure fluctuations and with comparatively minor changes in frequencies.

If we again use the measurements at  $x/H = 2.5$  and  $x/H = 1.0$  for zero open area ratio as reference values, we may plot the attenuation of the near field and far field as a function of open area ratio. Fig.19b suggests that quite small open area ratios (i.e. small amounts of ventilation) will strongly attenuate an acoustic resonance, even in a perforated working section with hard walls.

## 4.2 Flow unsteadiness in empty working sections

### 4.2.1 Closed working sections

Fig.20 shows the broadband pressure fluctuations measured along the sidewall of the closed working section with hard and laminate walls for some typical Mach numbers. If we consider first the pressure fluctuations at the choking Mach numbers ( $M_c = 0.85$  and  $0.90$  respectively with hard and laminate walls), we find that the pressure fluctuations, which must then propagate downstream from the settling chamber, are small, only about

$$\bar{P}/q = 0.3\% .$$

This confirms that the settling chamber design, with its honeycomb, three screens and contraction, is good.

At lower speeds the working section pressure fluctuations are higher, about

$$\bar{P}/q = 1.0\%$$

because pressure fluctuations can now propagate upstream from the diffuser. (The diffuser is generally the principal source of flow unsteadiness in a closed subsonic wind tunnel without a 'sonic throat'.) However, it is interesting to note that the working section pressure fluctuations with the laminate walls are generally lower than with the hard walls. This improvement can be related to the different wall characteristics if we examine the spectra of the pressure fluctuations for a typical point ( $x/H = 2.5$ ) for several speeds.

Fig.21 shows that when the working section is choked the flow unsteadiness with both walls at most frequencies is only about

$$\sqrt{nF(n)} = 0.001 .$$

However, at a frequency parameter corresponding with about 2200Hz, there is a peak of

$$\sqrt{nF(n)} = 0.003 \text{ with hard walls}$$

and only

$$\sqrt{nF(n)} = 0.002 \text{ with laminate walls.}$$

The difference occurs because the laminate walls provide a large attenuation at this frequency (Appendix). These peaks are caused by weak pressure fluctuations propagating downstream through the settling chamber from the reciprocating

compressors which drive the tunnel. (These compressors operate at a constant speed of 365rev/min  $\equiv$  2190Hz over the full speed range of the tunnel.) At lower speeds the peak at this frequency becomes more pronounced, e.g. at  $M = 0.60$  at 220Hz

$$\sqrt{nF(n)} = 0.010 \text{ with hard walls}$$

and only  $\sqrt{nF(n)} = 0.005$  with laminate walls.

The difference in this case occurs because the laminate walls also attenuate the pressure fluctuations generated by the compressors and which propagate upstream from the diffuser. In addition there is considerable unsteadiness, (about  $\sqrt{nF(n)} = 0.005$ ), at low frequency parameters ( $n = 0.01$  to  $0.04$ ). This low frequency unsteadiness is probably caused by relatively large scale separations in the diffusers and is unaffected by the change in wall material, because the laminate wall provides little attenuation at low frequencies in the range from 20 to 50Hz. (The measurements given in the Appendix extend down to 250Hz.)

The pressure fluctuations measured with the laminate and foam walls (omitted for clarity) are virtually identical. Hence the spectra for the laminate walls include no peaks which might be attributed to 'self noise' generated by the perforations in the PVC cover. A recent paper<sup>14</sup> showed that the 'self noise' generated by perforated liners backed with a honeycomb structure gave a Strouhal number based on hole diameter,  $d_h$ ; of

$$S^* = 0.2 ,$$

independent of the depth of the structure. If roughly the same Strouhal number applies to the perforations on the laminate there should be a peak in the unsteadiness spectra at a frequency parameter of about  $n = 0.2H/d_h = 13$ . However this would be well above the frequency response range of the measuring system, even at the lowest test speed,  $M = 0.30$ , and thus would not be observed.

We may infer that at  $M = 0.80$  the working section with hard walls is much closer to choking than with laminate walls (Fig.21) because the pressure fluctuations propagating upstream from the diffuser are appreciably smaller with hard walls than with laminate walls, both at high frequencies from the compressors and at low frequencies from the diffuser separations.

Some indication of the significance of these levels of flow unsteadiness and the changes produced by the wall material can be assessed by comparing the

measured spectra in Fig.21 with superimposed criteria developed for the detection of light buffeting (Ref.4, Fig.2). We will assume that the model chord is limited to

$$c = 0.1w ,$$

and we know that the buffet excitation covers the frequency range from  $f_c/u = 0.03$  to  $0.3$  at transonic speeds (Fig.12, Ref.15), which thus corresponds with  $n = 0.3$  to  $3.0$ . Hence the attenuation obtained at  $2200\text{Hz}$  with the laminate walls would be significant for buffeting tests.

#### 4.2.2 Slotted working sections

Fig.22 shows the broadband pressure fluctuations measured along the side-wall of the slotted working sections formed with hard, laminate or foam slats. The three typical Mach numbers selected illustrate interesting features of the measurements.

First we should notice that although the hard slats produce much higher pressure fluctuations in the working section than the laminate or foam slats, the driving pressure fluctuations generated in the extraction region at the end of the slats, are at a common level because the large scale mixing processes in this region are identical for the different slats. (See the discussion of the flow in the extraction region of a slotted working section given with respect to Figs. 24 and 27 of Ref.4). This common level can be inferred from the curves when extrapolated to  $x/H = 3.1$  (dotted in Fig.22) to be about  $\bar{P}/q = 1.2\%$  at  $M = 0.40$  and  $\bar{P}/q = 1.3\%$  at  $M = 0.80$ .

Now the measurements with the sound absorbing slats show only small variations with Mach number, but they are slightly different over the rear of the working section from  $x/H = 2.0$  to  $3.0$ . This small difference between the laminate and foam slotted liners is tentatively attributed to the fact that owing to a manufacturing error five of the twelve laminate slats have serrated streamwise edges. These, rough, serrated edges probably generate additional low frequency pressure fluctuations towards the end of the working section as an appreciable inflow extends into the slot.

The pressure fluctuations with laminate slats increase from about  $\bar{P}/q = 1.2\%$  at  $x/H = 3.0$ , reach a maximum at  $x/H = 2.5$  and remain constant at  $\bar{P}/q = 0.8\%$  to  $0.9\%$  from  $x/H = 1.5$  to  $0.5$ . With foam slats the corresponding pressure fluctuations are about  $\bar{P}/q = 1.1\%$  at  $x/H = 3.0$  and then fall steadily until they remain constant at  $\bar{P}/q = 0.8\%$  to  $0.9\%$  from  $x/H = 2.0$  to  $0.5$ . These levels of flow unsteadiness are better than most present transonic tunnels, but would not now be regarded as acceptable in new facilities.



In contrast, the pressure fluctuations measured with hard slats are higher and vary rapidly with Mach number. Thus at  $M = 0.80$  the pressure fluctuations increase from about  $\bar{P}/q = 1.6\%$  at  $x/H = 3.0$ , reach a maximum of about  $\bar{P}/q = 3.1\%$  at about  $x/H = 2.2$  and then decrease to a minimum of  $\bar{P}/q = 2\%$  at  $x/H = 1.5$ . The pressure fluctuations then increase to reach a second maximum of  $\bar{P}/q = 2.8\%$  at  $x/H = 0.5$ . This type of variation recalls the streamwise mode observed at lower speeds with both cylinders in the closed and slotted working sections with hard walls, e.g. Figs.7, 8, 12 and 14. There the excitation provided by the cylinder wake (at a shedding frequency,  $f^*$ , determined by the cylinder Strouhal number) was sufficient to force a streamwise mode within the working section at the frequency  $f^*$ . Here, the present measurements show (Fig.22) that the excitation provided at high subsonic and transonic speeds by the mixing region at the end of the liners (at a frequency determined generally by the slot width<sup>4</sup>) is also sufficient to force a streamwise mode within the working section. The modification of this streamwise mode by both the laminate and foam walls is clearly advantageous for dynamic tests at transonic speeds.

The insert in Fig.23 shows the broadband pressure fluctuations measured at  $x/H = 2.5$  over the full Mach number range of the tests. For this point the pressure fluctuations with both the laminate and foam slats are nearly constant from  $M = 0.3$  to  $0.8$ , at  $\bar{P}/q = 1.5$  and  $1.0\%$  respectively. This is a good feature of these working sections. In contrast the pressure fluctuations with the hard slats increase rapidly with Mach number to reach a maximum of  $\bar{P}/q = 3.4\%$  at  $M = 0.70$ . This large increase is a bad feature of this working section.

Fig.23 also shows the corresponding spectra for the typical Mach numbers. With the hard slats two broad peaks can generally be seen in the spectra. One corresponds with the compressor frequency of about 2200Hz, as in the closed work section (Fig.21) e.g. at  $n = 1.5$  for  $M = 0.40$ . However the level of this excitation is about three times higher than in the closed working section, and must therefore include some additional excitation or amplification from the extraction region. The peak at the lower frequency occurs at a frequency parameter of about

$$n = 0.5 \quad , \quad (\text{although not present at } M = 0.60)$$

and thus corresponds with a frequency parameter, based on the slot width  $w_s$ , of only about

$$n_s = 0.5 \times 0.034 = 0.017 .$$

This is low relative to the values previously observed in slotted working sections

$$n_s \cong 0.035 \quad (\text{Ref.4, Fig.25b}) .$$

With the sound absorbing slats all these peaks are attenuated and are more difficult to distinguish. It is encouraging to notice that the sound absorbing slats do significantly reduce the pressure fluctuations over a wide range down to frequencies as low as 150Hz over the full Mach number range, despite their restricted depth (only  $t = 13\text{mm}$ ). We would have expected the laminate liners to be superior to the foam liners from the wind off acoustic characteristics (Figs.29 and 30). However, the foam liners are superior to the laminate liners, possibly because of the serrations discussed above.

It is important to recall that the detailed design of transonic working sections has a decisive influence on the levels of flow unsteadiness achieved. Particular care is necessary in the design of the extraction region for tunnels with diffuser suction, as previous tests have already shown<sup>4</sup>. Some further evidence was provided during the present tests of the slotted working section with hard slats, and three examples of general interest are collated in Fig.24. The measurements all relate to  $x/H = 2.5$  and a Mach number of 0.60.

The sharp collector used for some preliminary tests excited an edge-tone at  $n = 0.6$  at this speed (Fig.24a). A bluff fairing placed under the sharp lip eliminated this edge-tone and thus reduced the excitation from  $\sqrt{nF(n)} = 0.02$  to 0.01. This edge-tone was comparable with that excited at the same speed by the diffuser collector in the perforated working section of the RAE 3ft  $\times$  3ft tunnel. The edge-tone in that perforated working section was also eliminated with a baffle (Ref.4, Fig.28).

The side plenum chambers of the 4in  $\times$  4in tunnel working section were left open during some preliminary tests to augment the small plenum chamber volume under the top and bottom liners. Although no mixing occurred along the side plenum chambers (because the sidewalls were closed throughout the experiment), the side plenum chambers were interconnected with the top and bottom plenum chambers and open at the rear to develop additional diffuser suction. A resonance occurred in the side plenum chambers at  $f = 550\text{Hz}$  ( $n = 0.26$ ) which corresponded closely with the closed/closed organ pipe mode for the plenum chamber

(Fig.24b). Rather than filling the side plenum chambers with solid materials, which would have drastically reduced the total plenum chamber volume, the side plenum chambers were partially filled with soft, open foam commonly used for packaging. This only slightly reduced the plenum chamber volume, but it suppressed the resonance and reduced the level of excitation in the working section from  $\sqrt{n^F(n)} = 0.025$  to 0.004.

Our discussion of the main measurements, made with the faired collector and the side plenum chambers filled as described, emphasised that the mixing in the extraction region and pressure fluctuations from the diffuser together were the main source of unsteadiness in slotted tunnels with diffuser suction. Hence it appeared likely that the pressure fluctuations in the working section could be reduced if the wind swept surfaces of the extraction region were lined with sound absorbing material. In the 4in x 4in tunnel it was only convenient to line a short streamwise length of the diffuser collector (55mm) to a depth of 13mm. (This modification was applied across the span of 115mm on all four walls.) The comparative measurements show that the application of this small area of sound absorbing material (laminar) in the most critical area of the diffuser reduced the level of pressure fluctuations in the working section from  $\sqrt{n^F(n)} = 0.015$  to 0.010 at about  $n = 0.9$  (Fig.24c).

In a future experiment the pressure fluctuations will be measured in the empty working section with much larger downstream areas of the diffuser covered with either laminar or foam. Further reductions in working section pressure fluctuations should then occur over a wider range of frequency, without any significant increase in the pressure ratio required to drive the tunnel. (The tunnel pressure ratio is determined primarily by the large losses caused by the sudden expansion in the extraction region, and is relatively insensitive to changes in the boundary layer profiles on the walls of the diffuser.)

Comparative measurements showed that none of the modifications described in Fig.24 had any significant effect on the pressure fluctuations generated by the circular cylinders at the shedding frequency over the Mach number range from  $M = 0.3$  to 0.5, although there were significant changes in the level of flow unsteadiness in the empty tunnel, particularly at  $M = 0.50$ .

#### 4.2.3 Perforated working section

Fig.25 shows that the measured pressure fluctuations in the perforated working section are generally similar in character and level with those for the closed working sections with hard walls (section 4.2.1). The broadband pressure

fluctuations are about  $\bar{P}/q = 0.6\%$  to  $0.9\%$  and show some variation along the working section. (Compare Figs.25 and 20). The spectra at the typical point considered ( $x/H = 2.5$ ) are almost identical with those in the closed working section with hard walls (compare Figs.26 and 21).

In the low Mach number range from  $M = 0.2$  to  $0.3$ , the absence of a peak in the spectra at the appropriate frequency parameter ( $n = 5.4$  based on tunnel width), suggests that the  $0.79\text{mm}$  diameter  $60^\circ$  inclined holes do not generate edge-tones. This observation is consistent with the previous measurements<sup>4</sup>. Hence to develop edge-tones it may be necessary to satisfy some other condition(s) in addition to having,

$$\delta^*/d > 0.5$$

as previously suggested<sup>4,16</sup>. (For the present tests rough estimates show that  $0.5 \leq \delta^*/d \leq 1$  .

## 5 DISCUSSION

The experiments described above show, as hoped, that the replacement of the hard walls of a small conventional wind tunnel by sound absorbing walls eliminates resonances excited by circular cylinders, and reduces the level of flow unsteadiness.

We must now ask if effects similar in character might be expected with other models, which would thus justify the incorporation of sound absorbing walls in a larger facility. Before answering these questions we must look more closely into the resonance phenomenon.

The resonances excited by the circular cylinders in the closed working section with hard walls, when the vortex shedding frequency coincides with the predicted transverse frequency, were extremely large (Figs.7 and 8) and imply a dramatic change in the vortex shedding. We know from a previous experiment<sup>17</sup> that, at resonance, vortex shedding occurs strictly in phase over the complete span of the cylinders, so that the level of pressure fluctuations becomes very large\*. Sound absorbing walls introduce attenuation and possibly a change of

---

\* Similarly the sound generated by the flow past a circular wire increases dramatically when the vortex shedding coincides with the first natural vibration frequency of the wire. The large amplitude motion of the wire then ensures that the phase of the large eddies loses its randomness along the wire, so that the correlation distance increases suddenly towards the full length of the wire<sup>18</sup>.

phase along the boundaries of the working section altering the feedback process. Hence it may be difficult to excite a resonance and vortex shedding may not occur strictly in phase across the cylinder. In an unconfined flow ( $H \equiv \infty$ ) the vortex shedding on a circular cylinder is only strongly correlated<sup>19</sup> over a spanwise length of about  $3d$ . If this correlation length is used, the pressure fluctuations on the mid-plane of the cylinder ( $Z \equiv 0$ ) corresponding with the measurement stations in the working section (along the line  $y = -H/2$ ) may be estimated according to the theory given in Ref.19. (Estimates from this theory agreed reasonably well with measurements made on a small cylinder in a large low speed tunnel<sup>19</sup>.) Fig.27 shows that these estimates also agree fairly well with the present measurements made in the side wall of the small closed working section, when the resonances are suppressed by the sound absorbing walls. The agreement at  $M = 0.24$  is fair. However the agreement at  $M = 0.40$  should be viewed with caution because the cylinder is now approaching the critical Mach number in the unconfirmed flow (when the theory would be invalid) and the blockage (18%) might be expected to spoil the comparison. The sensitivity of the estimates to blockage can be gained from low speed experiments<sup>20</sup>, which covered a range of blockage from 5 to 35% at Mach numbers up to  $M = 0.15$ . These measurements gave the following blockage corrections for two-dimensional circular cylinders:

for rms lift coefficient  $\bar{C}_L = (\bar{C}_L)_{\text{unconfined}} / (1 - 1.95d/H)$

and

for Strouhal number  $S^* = (S^*)_{\text{unconfined}} / (1 - 0.55d/H)$ .

When these blockage corrections are applied to the estimated pressure fluctuations for the unconfined flow (dashed curves), the pressure fluctuations for the confined flow are obtained (dotted curves). The measurements and the estimates with the blockage correction are in good agreement at  $M = 0.24$ , whereas at  $M = 0.40$  the measurements are bracketed by the estimates. (It will be noticed that the high blockage correction at  $M = 0.40$  is consistent with the high Strouhal number measured.) Hence it is likely that when acoustic resonances are suppressed we have a fair approximation to interference free flow.

It is interesting to note that the measured pressure fluctuations for the 18mm diameter cylinder at  $M = 0.40$  in both the hard slotted (Fig.14) and perforated working sections (Fig.18) agree with those in the closed working section with laminate walls (Fig.9) and hence with the estimates (Fig.27). This suggests that ventilated walls, even made from hard materials, may modify resonance conditions by altering the boundary condition for reflected waves, and hence the degree of spanwise correlation of the vortex shedding. (The previous

discussion of Figs. 16 and 19 may also be recalled.) The poor estimates (given at Fig. 2b) for the resonance frequencies in the slotted working section used for the present experiment may also be attributed to an over-simplified boundary condition at the wall. The theory<sup>8</sup> assumes that the volume behind the slots is infinite, whereas it is quite small. The theory also makes no allowance for the impedance of the flow through the slots, which may be significant for the deep slots used here. The theory works well for closed working sections because the boundary conditions are then precisely defined. Previous tests have indeed shown that two-dimensional<sup>21,22</sup> and three-dimensional<sup>23</sup> models oscillating in pitch excite resonances in closed working sections at the predicted<sup>8</sup> resonance frequencies.

From this discussion we may infer that other models having oscillatory motion (at an appropriate tunnel resonance frequency) strongly correlated in space and time are most likely to excite resonances. Thus a two-dimensional aerofoil oscillating in pitch is more likely to excite a resonance than a three-dimensional wing with an oscillating flap partially spanning the trailing-edge, because the pressure fluctuations on the two-dimensional aerofoil are strongly correlated over a much larger area. Similarly, we would expect that resonance phenomena will be potentially more serious for the primary bending or torsional modes on an aeroelastic model, than for overtone modes which have smaller correlation lengths. Again, we would *a priori* expect that resonance phenomena might be more serious for a flutter-test than for a buffeting test because the pressure fluctuations which excite buffeting are generally independent of the motions of the structure, are correlated over smaller lengths and cover a wide frequency band<sup>15</sup>. Hence appropriate sound absorbing walls may certainly be preferred to hard walls for transonic tests of two-dimensional aerofoils or for flutter measurements. There may also be some gains for both flutter and buffeting measurements consequent upon the lower levels of flow unsteadiness associated with sound absorbing walls.

It is likely that the acoustic characteristics of the wall material required are not critical, as long as a reasonable degree of attenuation (say  $\alpha_r \geq 0.5$ ) is provided over the frequency range within which resonance is expected, as in the present tests, see Appendix and Figs. 29 and 30). Indeed the final choice of wall material for a transonic working section which is to suppress resonances might be decided as the result of a compromise between acoustic properties, cost, durability and any additional boundary layer growth relative to a hard wall. This last factor might be particularly important in a

continuously operated fan driven tunnel, where a small increase in pressure ratio implies a large increase in the fan-power.

In contrast, the acoustic characteristics of the wall material will be crucial if a specified level of flow unsteadiness (say  $\sqrt{nF(n)} \leq 0.002$  as suggested previously<sup>4</sup>) is to be attained in the empty tunnel over a given frequency range at a particular speed. This objective may be attained by first minimizing the flow unsteadiness generated in a conventional working section with hard walls (e.g. by choosing a larger number of narrow slots, careful design of the extraction region, plenum chamber and diffuser) and then by introducing sound absorbing walls wherever appropriate. In particular, large reductions in flow unsteadiness may be obtained by using sound absorbing materials for the slats of a slotted working section (section 4.2.2). These large reductions are not constant along the working section and correspond with the suppression of a forced acoustic mode, rather than orthodox sound attenuation along a duct, which can generally be expressed in terms of decibels/unit length. In a dynamic test section currently being considered for the RAE 3ft x 3ft tunnel a low level of unsteadiness is desired at all frequencies, but especially in the range from 250 to 1000Hz. Laminate slats with a depth of 50mm have been provisionally selected to meet this requirement (Fig.30).

The present tests have not included any formal assessment of the performance of sound absorbing walls for wind tunnels at supersonic speeds. This is not a serious limitation because resonances, the main concern at subsonic and low transonic speeds, cannot be maintained in the working section at supersonic speeds and because the flow unsteadiness is generally much lower at supersonic speeds. However, dynamic interference can still occur whenever unsteady shock or expansion waves from the model are reflected by the tunnel walls back onto the model. Such reflection will occur from transonic working sections with hard walls at high transonic speeds, say from  $M = 1.0$  to 1.3. In this speed range the sound absorbing walls should still offer significant reductions in dynamic interference.

This hypothesis is confirmed by some recent tests\* made by firing rifle bullets between top and bottom liners removed from the pilot tunnel. The liners

---

\* These tests were kindly made at the author's request by Dr. L. Pennelegion, in a firing range at the Royal Military College of Science at Shrivenham. The round has a calibre of 7.62mm and a length of 27mm; for the test illustrated it travels at  $M = 1.7$ . The photographs were taken with a divergent shadow-graph system and have a spark duration of about 1 $\mu$ s. The spark system is activated when the bow shock vibrates a 'trembler plate' set an appropriate distance upstream, and below, the working section.

are held 50mm apart so that the reflected bow wave clears the base of the round (Fig.28).

The top liner is closed and hard. It provides a reference for the performance of the bottom liner, made from sound absorbing material. Fig.28a shows that the foam wall almost completely cancels the moving shock waves of widely varying strength which emanate from the bluff nose, the rifling and the recompression fan from the closure of the wake downstream of the base bubble. Fig.28b shows that the laminate wall has the same general tendency, but is less effective. Fig.28c shows the normal, unconfined flow in the range, which closely corresponds with the lower half of Fig.28a. Although Fig.28 refers to the closed liners, virtually identical results were obtained with slotted liners. The same trend of shock wave cancellation with changes in wall material was observed at higher speeds ( $M = 2.5$ ) and could be expected at low supersonic speeds\*. Hence we may expect significant reductions in dynamic interference with these walls even in the high transonic speed range. These remarks refer to dynamic interference at high frequencies. At low frequencies the sound absorbing walls might be expected to diffuse incident shock waves, rather than attenuating them. This aspect of their performance may be investigated in a further experiment in the 4in  $\times$  4in tunnel.

This discussion suggests that sound absorbing walls of this type offer significant advantages for tests of relatively large dynamic models in wind tunnels at subsonic and transonic speeds<sup>27</sup>. The improvements possible may be assessed more fully by comparative tests of an oscillating model in a larger facility with alternative walls. Tests of this type in a modified working section for the RAE 3ft  $\times$  3ft tunnel are being considered.

## 6 CONCLUSIONS

Comparative tests of circular cylinders operating in the subcritical Reynolds number range in specially designed closed and slotted working sections with alternative hard, laminate and foam walls show that the wall material strongly influences the pressure fluctuations generated. In particular, both the laminate and foam walls suppress resonance phenomenon which occur with hard walls which would not be present in the unconfined flow.

---

\* Wurzel and Hottner have shown rather similar photographs<sup>24,25</sup> for revolver bullets moving at speeds from  $M = 1.2$  to 1.3 with different types of compliant wall materials. Spark photographs taken by Sabol for a bullet travelling at  $M = 1.1$  also showed that 19mm thickness of cotton batting could completely cancel moving shock waves (Ref.26, Fig.15).



Comparative tests in the empty closed and slotted working sections also show that both the laminate and foam walls reduce the level of flow unsteadiness relative to that observed with hard walls. In the slotted working section at transonic speeds these reductions are large.

These preliminary tests in the pilot 4in  $\times$  4in tunnel are judged sufficiently encouraging to justify further investigation at a larger scale in the RAE 3ft  $\times$  3ft tunnel, which it is hoped will include tests of an oscillating model.

#### Acknowledgments

The author would like to acknowledge some assistance from the staff of the Wolfson Unit for noise and vibration research at Southampton University. Mr. R.D. Rawlinson made the measurements described in the Appendix and Prof. P. Doak made informal comments on the pilot tunnel experiments.

Appendix

PROPERTIES OF WALL MATERIALS

The sound absorbing walls selected for these tests are commercially available\* open-celled polyether foams. These are resistant to oils and solvents, do not support mould growth or vermin and are also non-inflammable. These physical properties are considered advantageous for a material intended for use in large wind tunnels. The density of the foam specimens tested is about  $27\text{kg/m}^3$ . The laminate is formed by bonding a thin layer of perforated PVC to one side of a foam sheet. The perforations are circular holes with a diameter of only 1.58mm, and are drilled on a square grid with sides 3.22mm long; this gives an open area ratio of about 19%. It is interesting to notice that these flexible polyether foams have mechanical properties generally resembling those of the flexible polyurethane foams which have been tested in attempts to reduce the drag of turbulent wall boundary layers<sup>28</sup>.

The manufacturer's specification offered significant sound absorption in still air in the wide frequency range of interest, from 250 to 2500Hz. However, it was considered essential to obtain some independent acoustic measurements from the samples actually tested because fairly wide local variations sometimes occur, even with a single sheet of this material. In addition the manufacturer's specification did not include any data for sheets of only 13mm thickness, as used in the slats of the slotted working section. Accordingly some absorption coefficients were measured<sup>29</sup> at the Institute of Sound and Vibration Research using a Brüel and Kjaër wave impedance tube, type 4002.

The normal incidence coefficients actually measured are shown in Fig.29; the corresponding random incidence coefficients, derived from the Brüel and Kjaër correction chart, are shown in Fig.30. The random incidence coefficient is more generally presented and although the non-uniformity of the foams and the difficulty of ensuring a close fit of the laminate round the sides of the tubes, caused some uncertainty, Fig.30 should give a fairly accurate indication of the sound absorption coefficients of the walls.

Fig.30a shows that at a thickness of only 13mm (as used with the slats) the laminate has an appreciably higher absorption coefficient than the foam up to about 1000Hz, but that above this frequency the difference between the two curves diminishes rapidly. Fig.30b shows that at an increased thickness of 25mm (as

---

\* Supplied by: Pritex (Plastics) Ltd.,  
 Wellington,  
 Somerset.

used in the closed working sections) the laminate clearly maintains its advantage over the foam up to a frequency of 2000Hz. The pressure fluctuation measurements given in Figs.9 and 10 suggest that acoustic resonances can just be suppressed by the foam at a frequency of 1500Hz, which corresponds (Fig.30b) to a minimum absorption coefficient of about

$$\alpha_r = 0.5 .$$

If we accept this rough criteria, Fig.30c suggests that a 50mm thickness of laminate should also eliminate all resonances between 250Hz and 2500Hz, which would satisfy the design condition for the full scale, 3ft tunnel working section. The increase in thickness of the laminate from 25mm to 50mm makes a big improvement at low frequencies (as required) at the expense of some degradation at high frequencies (which is relatively unimportant).

The measurements in Fig.30 are intended to give an indication of the wall characteristics required for a successful wind tunnel application of this concept, and all refer to zero speed. Some rough idea of the possible influence of flow on the laminate may be gleaned from attenuation measurements<sup>30</sup> in a duct lined with thin perforated sheet (of unspecified open area ratio) backed by a 75mm thickness of Rockwool. These measurements (Fig.17, Ref.30) show at  $M = 0$  similar spectra to the measurements given in Fig.30c for the laminate with  $t = 50\text{mm}$ . As speed increased from  $M = 0$  to  $M = 0.4$ , Fig.17, Ref.30 shows that the attenuation increased for sound waves moving upstream. Fig.16, Ref.30 shows that the attenuation decreased for sound waves moving downstream. Hence, *a priori*, rather similar trends might be expected for the laminate, as long as 'self-noise' effects are excluded.

Finally it is interesting to note that the mechanical properties of the laminate are apparently not seriously altered by variations in temperature between about 100 K to 370 K. With a view to a possible application in lining the circuit or forming the slotted or closed working section of a cryogenic transonic tunnel, a sample of the laminate was immersed seven times in liquid nitrogen. After every immersion no trace of differential expansion between the foam and the PVC was observed. However, some loss of flexibility, and hence in sound absorption properties, must be expected at very low temperatures. The low thermal conductivity of the foam [only  $0.036\text{W/m}^{\circ}\text{C}$  ( $0.25\text{Btu/in/ft}^2\text{h}^{\circ}\text{F}$ ) at room temperatures and less at lower temperatures] could make the laminate an effective insulator for lining a cryogenic tunnel. This could reduce both the time taken to establish steady conditions and the cooling nitrogen requirements to maintain

## Appendix

steady conditions. Gaseous nitrogen absorbed during the tunnel run by the open-cell structure of the foam should diffuse away quickly when the tunnel was vented to the atmosphere. This possible application of the laminate in cryogenic wind tunnels appears worth studying, if the foam can be permanently bonded to the tunnel shell.

SYMBOLS

$\bar{C}_L$	rms fluctuating lift coefficient
$\bar{C}_D$	rms fluctuating drag coefficient
c	model chord
$C_f$	local skin friction coefficient
d	cylinder diameter (m)
f	frequency (Hz)
f*	vortex shedding frequency (Hz)
$f_r$	predicted tunnel transverse resonance frequency (Hz)
F(n)	spectrum function
H	tunnel height (m)
M	Mach number
$M_c$	choking Mach number
$n = fw/u$	frequency parameter
$\bar{p}$	rms pressure fluctuation in narrow bandwidth $\epsilon f$ ( $N/m^2$ )
$\bar{P}$	broadband rms pressure fluctuations ( $N/m^2$ )
$\overline{p^2}$	mean square pressure fluctuation ( $N^2/m^4$ )
q	kinetic pressure ( $N/m^2$ )
R	free stream unit Reynolds number (/m)
$S^* = f*d/u$	Strouhal number
u	free stream velocity (m/s)
w	tunnel width (m)
x,y,z	rectangular coordinates of point relative to origin on horizontal centre line of tunnel, shown in Fig.1
$\alpha_0$	normal incidence sound absorption coefficient
$\alpha_r$	random incidence sound absorption coefficient
$\delta^*$	boundary layer displacement thickness (m)
$\epsilon$	analyser bandwidth ratio (%)

REFERENCES

<u>No.</u>	<u>Author</u>	<u>Title, etc.</u>
1	W. Sears	Self correcting wind tunnels. Aeronaut. J. Vol.78, pp.80-89, Feb/March 1974
2	C.L. Ruhlin R.A. Gregory R.M. Destuynder	Some tunnel wall effects on transonic flutter. AIAA Paper 74-406, April 1974
3	K.W. Newman C.W. Skingle D.R. Gaukroger	The development of rapid-testing techniques for flutter experiments. ARC CP No.1274 (1973)
4	D.G. Mabey	Flow unsteadiness and model vibration in wind tunnels at subsonic and transonic speeds. ARC CP 1155 (1971)
5	J.P. Hartzuiker P.G. Pugh W. Lorenz-Meyer G.E. Fasso	On the flow quality necessary for the large European high Reynolds number transonic wind tunnel LEHRT. AGARD Report 644, March 1976
6	A. Naumann	Uber einige probleme der aerodynamischen grundlagenforschung. Zeit. Flügwiss, Vol.7, Part 2, pp.203-217, July 1961
7	E. Achenbach	Influence of surface roughness on the cross flow around a circular cylinder. J. Fluid Mech. Vol.46, Part 2, pp.321-335 (1971)
8	W.E.A. Acum	A simplified approach to the phenomenon of wind tunnel resonance. ARC R & M No.3371 (1962)
9	G.M. Lilley	On wall pressure fluctuations in turbulent boundary layers. ARC 24241 (1962)
10	R.H. Wright V.S. Ritchie	Characteristics of a transonic test section with various slot shapes in the Langley 8ft high speed tunnel. NACA Report 1389 (ARC 14844)
11	E.J. Richards D.J. Mead	Noise and acoustic fatigue in aeronautics. Chapter 2, pp.43-72, Wiley (1968)

REFERENCES (continued)

<u>No.</u>	<u>Author</u>	<u>Title, etc.</u>
12	P.E. Doak	Excitation, transmission and radiation of sound from source distributions in hard-walled ducts of finite length. Part 1 Effects of duct cross-section geometry and source distribution space-time pattern. J. Sound Vibrat., 31(1), pp.1-72 (1973)
13	P.E. Doak	Excitation, transmission and radiation of sound from source distributions in hard-walled ducts of finite length. Part 2 The effects of duct length. J. Sound Vibrat., 31(2), pp.137-174 (1973)
14	A.B. Bauer R.C. Chaphis	Noise generated by boundary layer interaction with perforated acoustic liners. AIAA Paper 76-41, January 1976
15	D.G. Mabey	Beyond the buffet boundary. Aeronaut. J. Vol.77, pp.201-215, April 1973
16	G.F. McCanless	Noise reduction in transonic tunnels. J. Acoust. Soc., America, Vol.56, No.5, pp.1501-1510 (1974)
17	M. Gaster	Some observations on vortex shedding and acoustic resonances. ARC CP 1141 (1971)
18	O.M. Phillips	The intensity of Aeolian tones. J. Fluid Mech., Vol.1, Part 6, pp.607-624, December 1956
19	B. Etkin G.K. Korbacher R.T. Keefe	Acoustic radiation from a stationary cylinder in a fluid stream. UTIA Report 39, May 1956, also J. Acoust. Soc. America, Vol.29, No.1, pp.30-36 (1957)
20	Saad el-Sayed el Sherbiny	Effect of wall confinement on the aerodynamics of bluff bodies. PhD. Thesis, University of British Columbia, September, 1972

REFERENCES (concluded)

<u>No.</u>	<u>Author</u>	<u>Title, etc.</u>
21	H.L. Runyan D.S. Woolston A.G. Rainey	Theoretical and experimental investigation of the effect of tunnel walls on the forces on an oscillating airfoil in two-dimensional subsonic compressible flow. NACA Report 1262 (1956)
22	W.P. Jones	Wind tunnel wall interference effects on oscillating aerofoils in subsonic flow. ARC R & M No.2943 (1957)
23	E. Widmayer S.A. Clevenson S.A. Leadbetter	Some measurements of aerodynamic forces and moments at subsonic speeds on a rectangular wing of aspect ratio 2 oscillating about the mid-chord. NACA TN 4240, May 1958
24	D. Wurzel	Experimental study of suppression of unsteady shock waves with 'elastic walls'. Unpublished diploma in the University of Stuttgart, October 1974
25	T. Hottner	Wandinterferenzprobleme im hybridkanal bei transsonischen geschwindigkeiten. Chapter 9, Year Book of DGLR, DGLR 76-169 September 1976
26	A.P. Sabol	A preliminary investigation of shock-wave reflections in a small closed ballistic range with various types of walls. NACA RM L52 G25, (NACA/TIB 3348), September 1952
27		Draft Patent Application Number 21730/76 dated 26 May 1976
28	K.W. McAlister T.M. Wynn	Experimental evaluation of compliant surfaces at low speeds. NASA TM X-3119, October 1974
29	I. Sharland	Woods Practical Guide to Noise Control, pp.50 and 51. Published by Woods (1972)
30	Anon	Research on sound propagation in sound absorbent ducts. USAF AMRL TDR 62-140 Part 2, December 1962



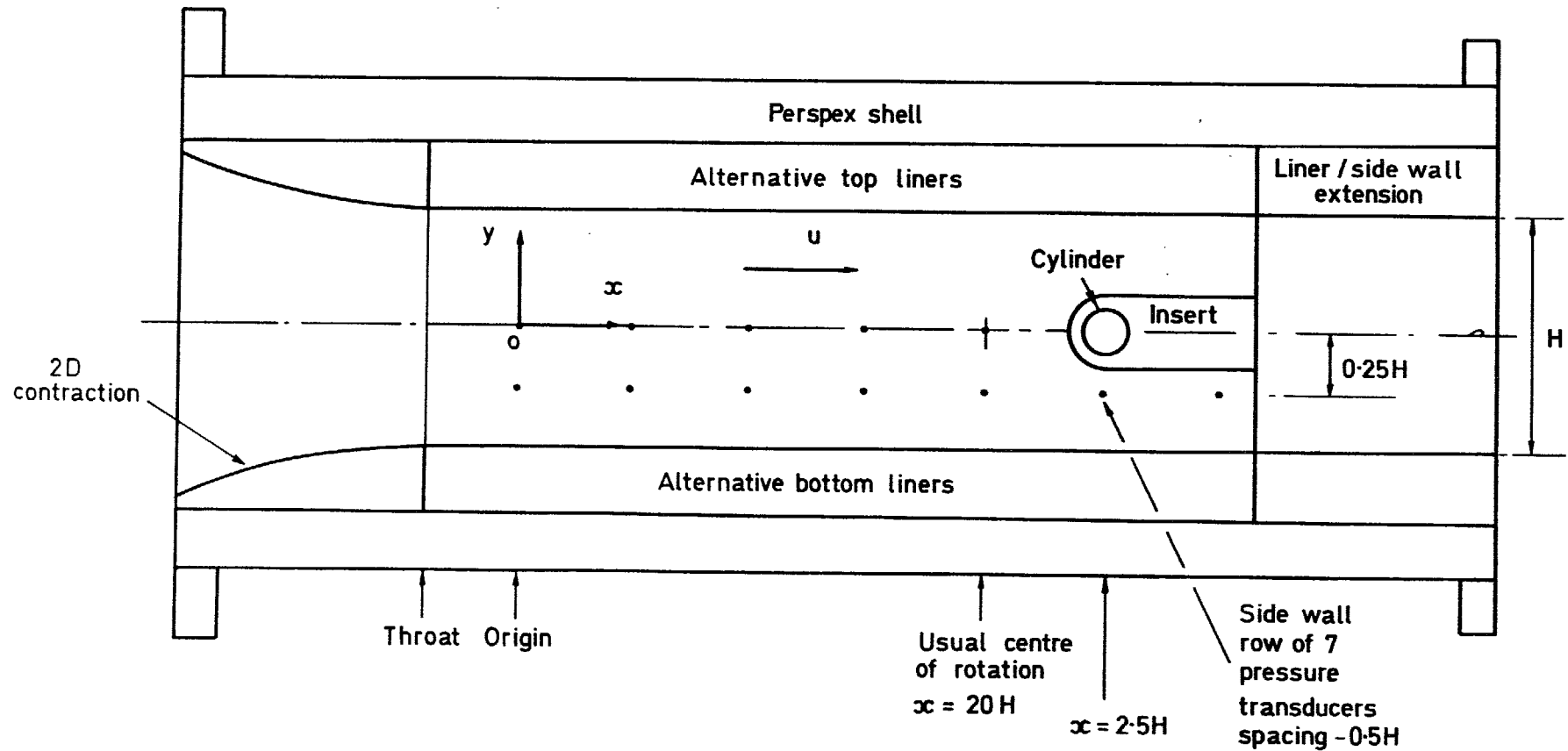


Fig 1 GA of circular cylinder in 4in x 4in tunnel – (closed working section illustrated)

Fig 2a&b

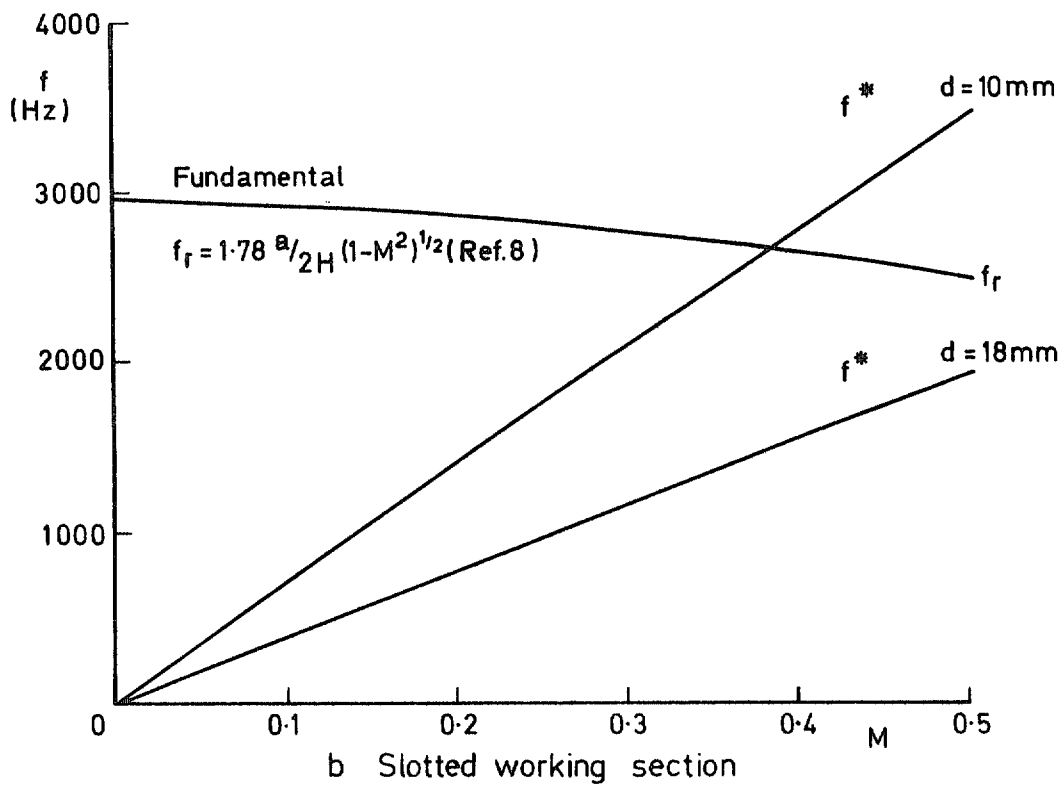
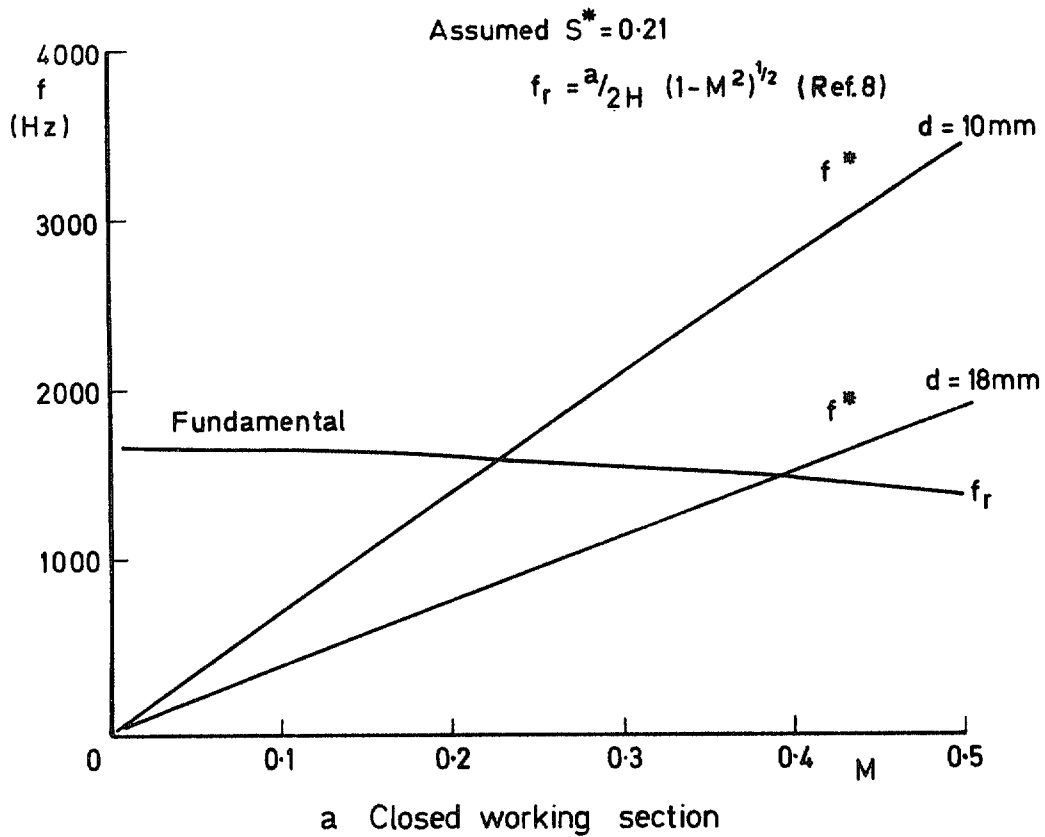
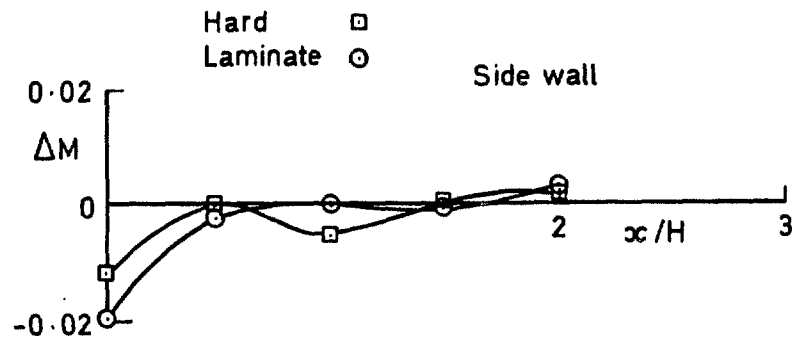
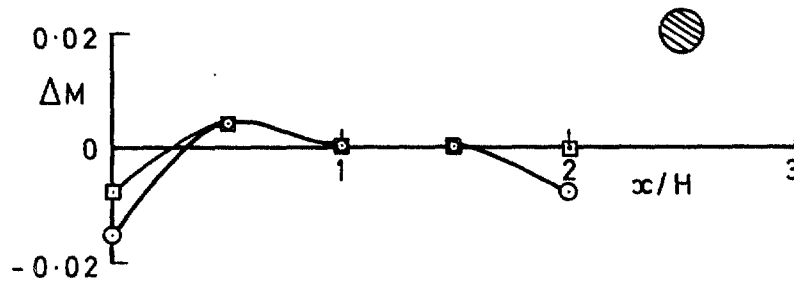


Fig 2a&b Predicted shedding ( $f^*$ ) and resonance frequencies ( $f_r$ )



a Tunnel empty



b  $d = 18\text{mm}$

Fig 3a&b Mean Mach number distributions —  $M = 0.4$ . Closed working sections

Fig 4a&b

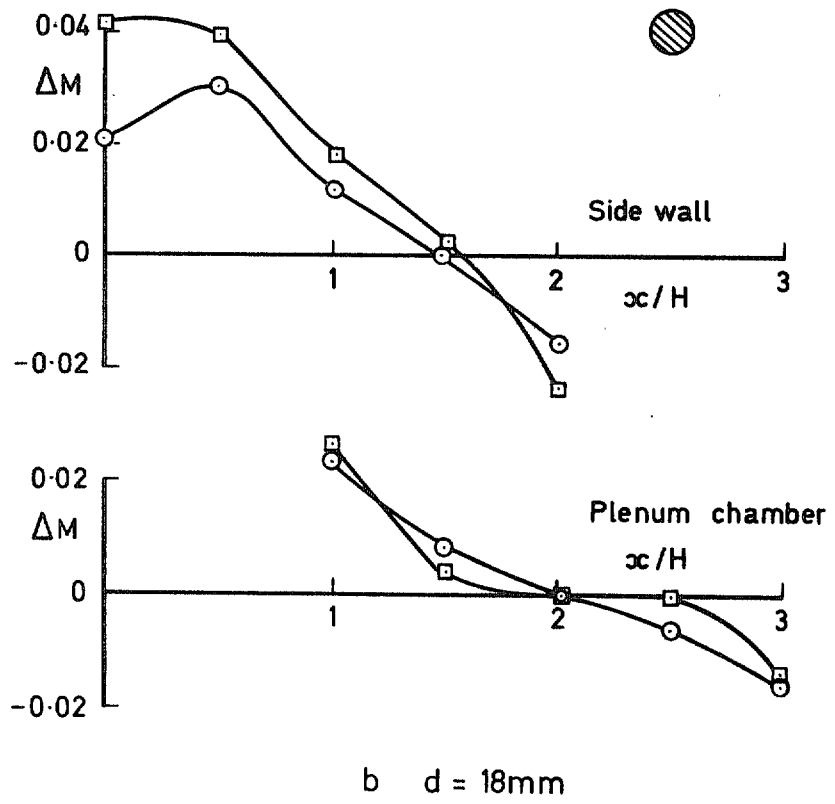
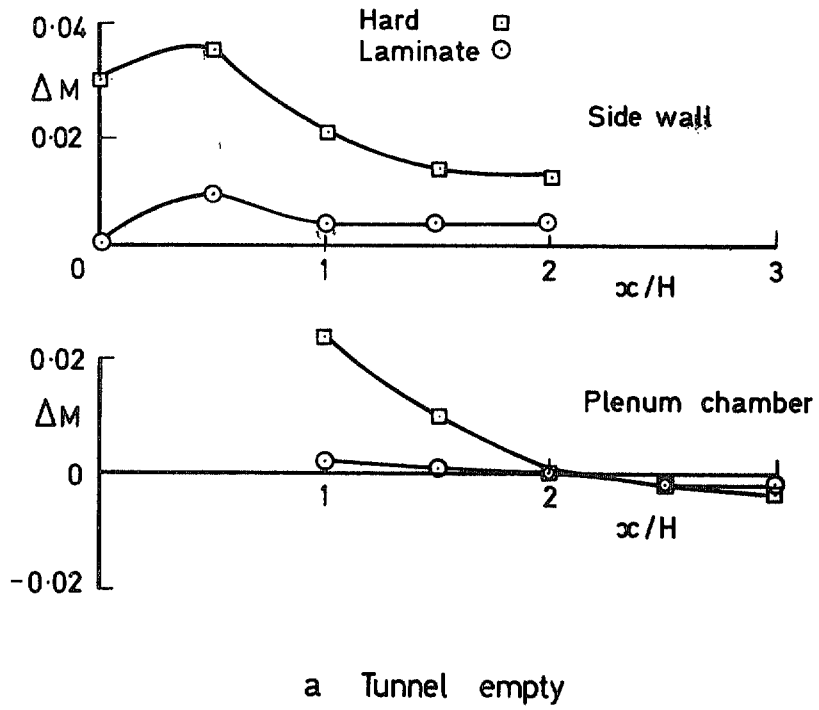
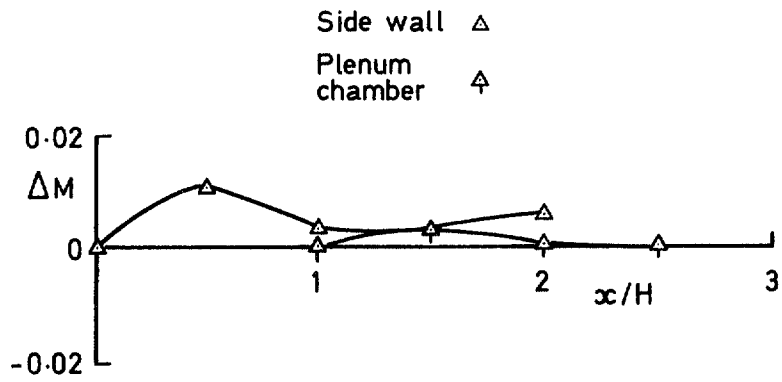
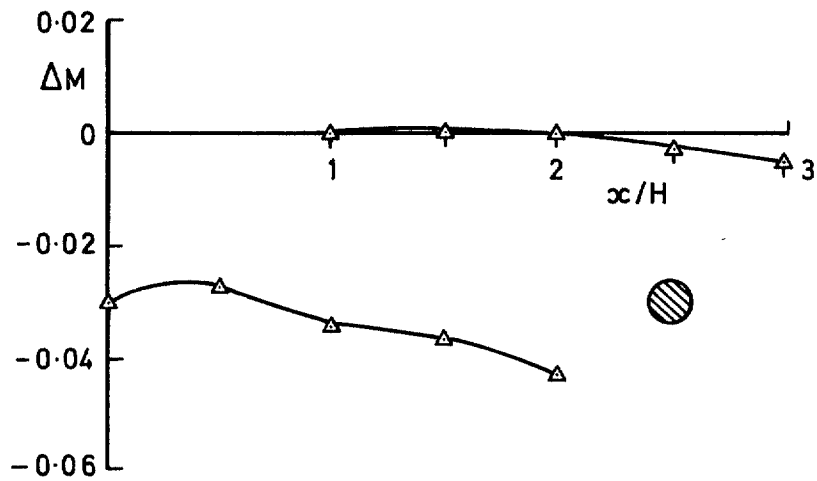


Fig 4a&b Mean Mach number distributions —  $M = 0.4$ . Slotted working sections

Fig 5a&b



a Tunnel empty



b  $d = 18\text{mm}$

Fig 5a&b Mean Mach number distributions —  $M = 0.4$ . Perforated working sections

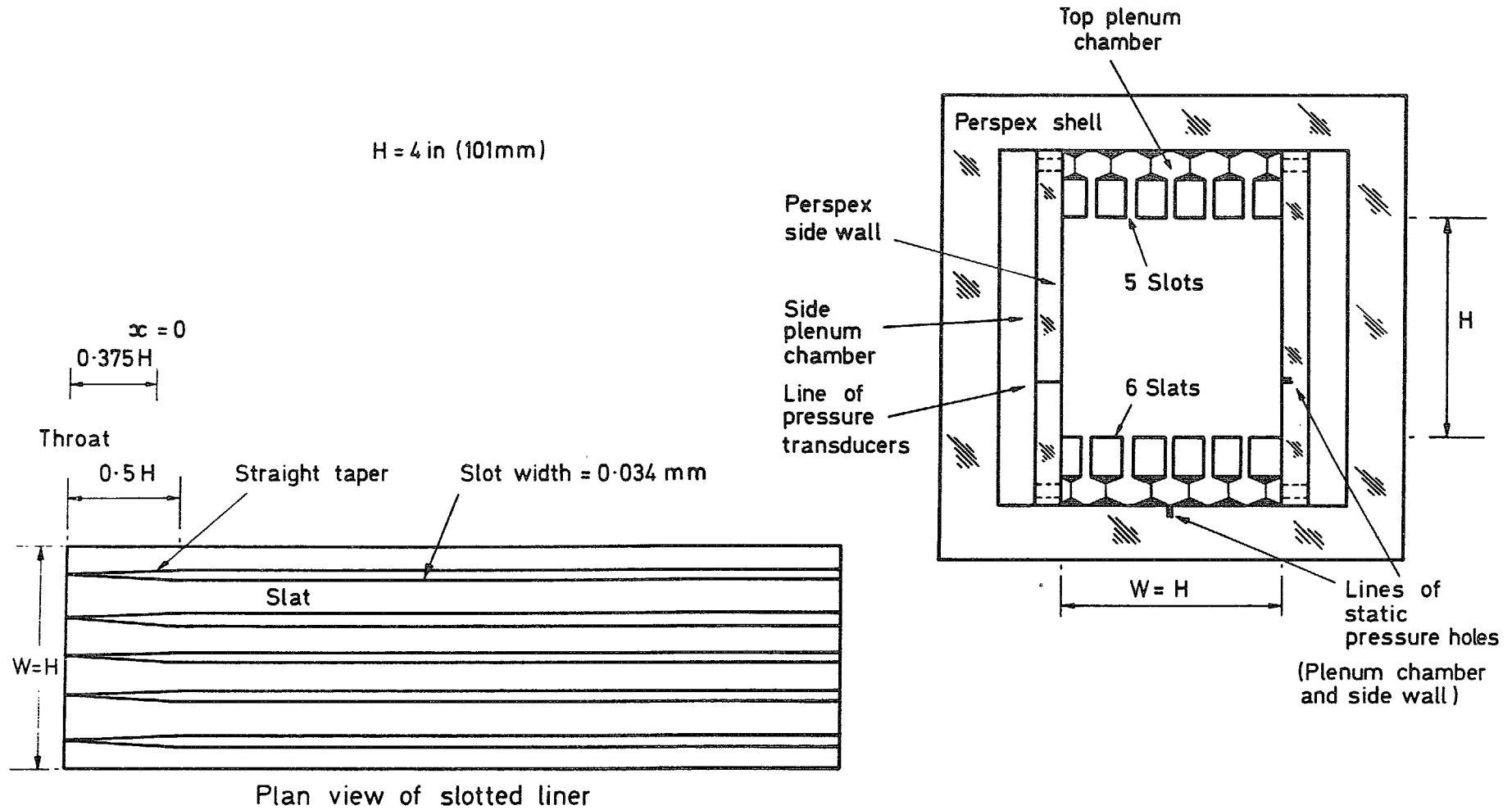


Fig 6 Details of slotted working section for 4in x 4in tunnel

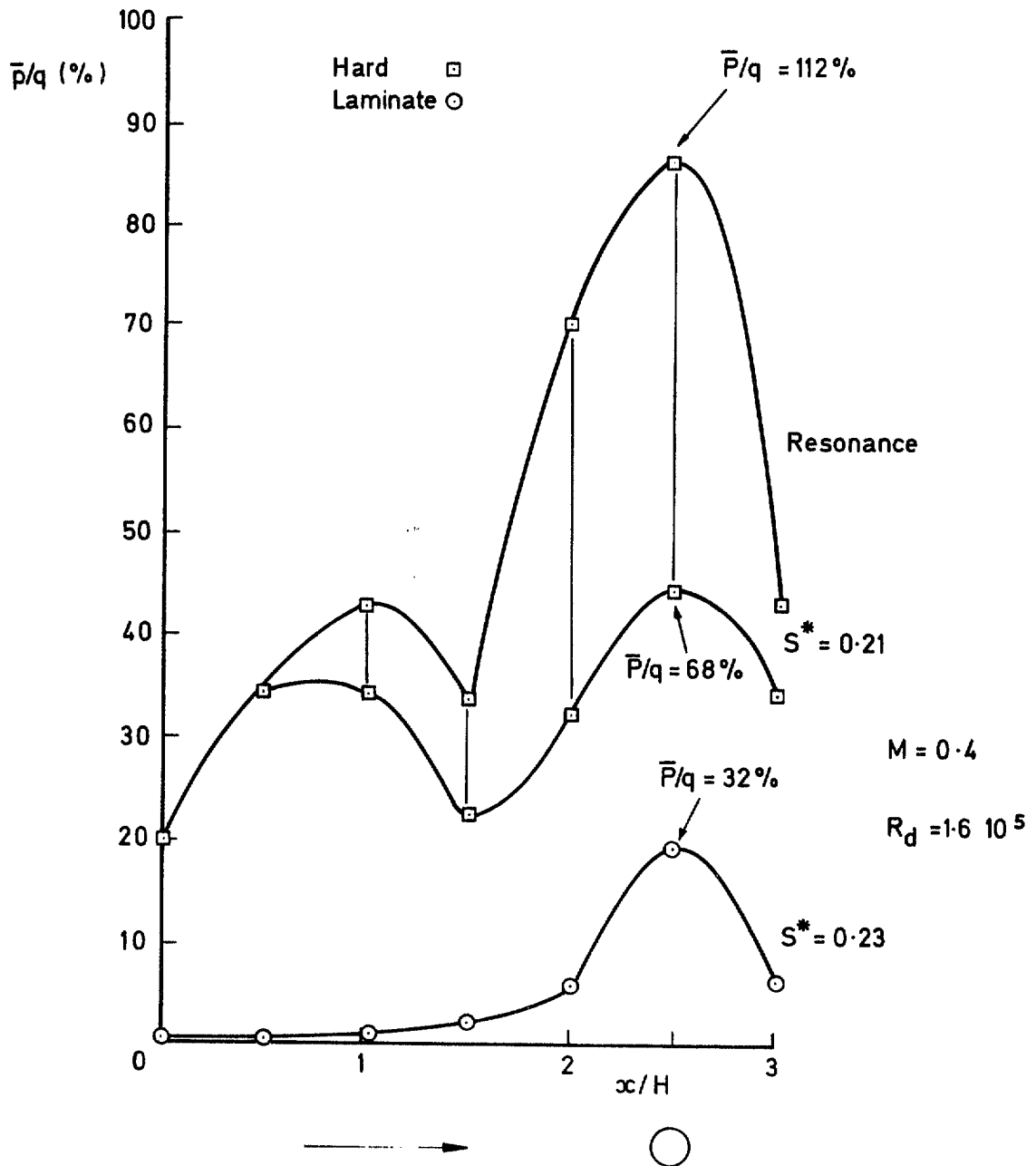


Fig 7 Interference in closed working sections:  $d = 18$  mm, two wall materials

Fig 7 contd

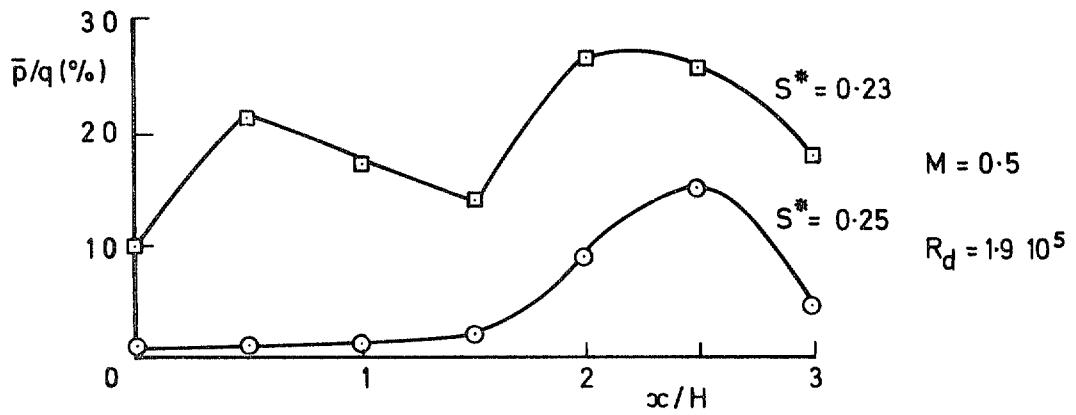
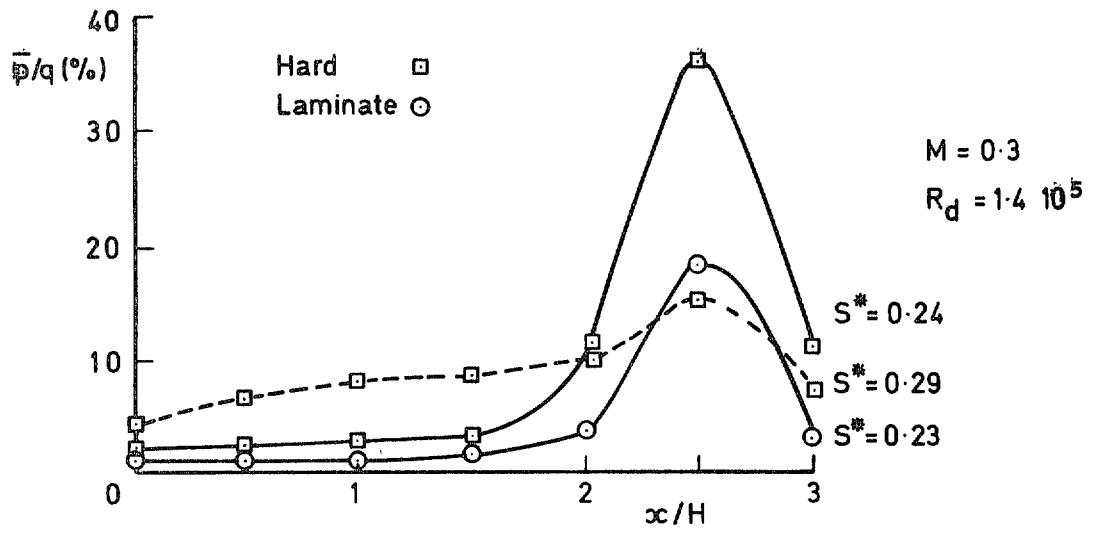


Fig 7 contd



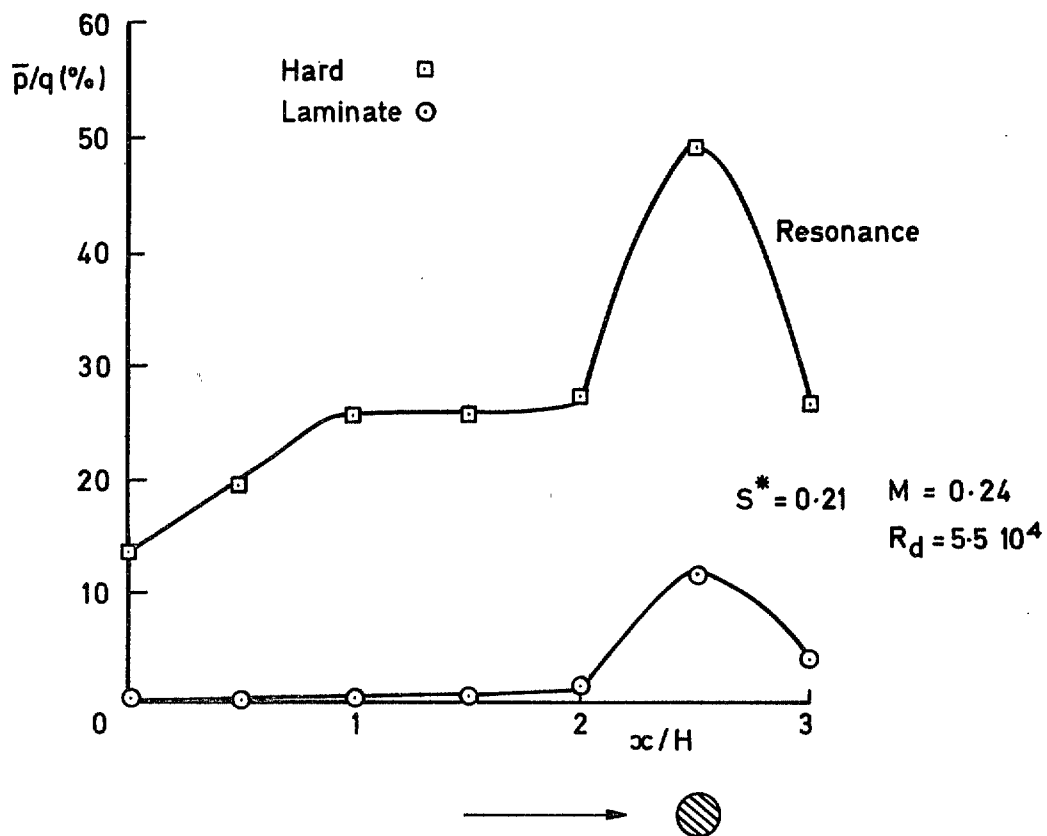


Fig 8 Side wall pressure fluctuations showing interference in closed working sections for  $d = 10$  mm and two wall materials

Fig 8 contd

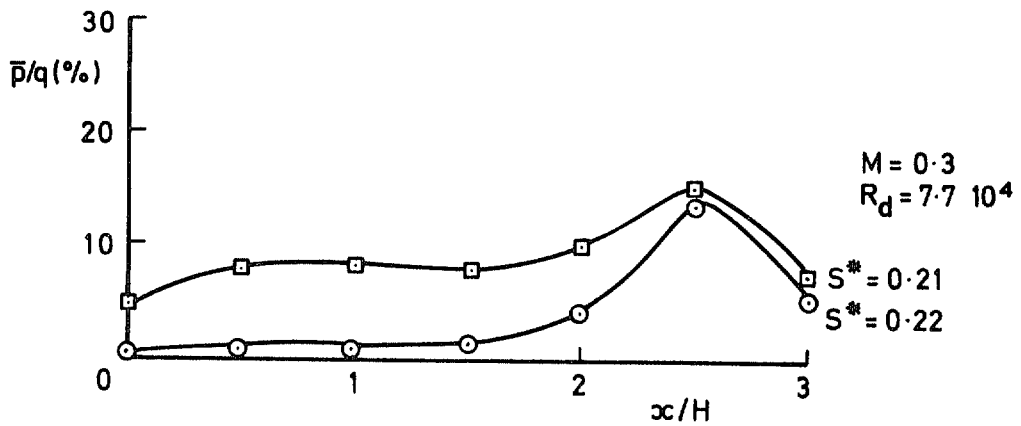
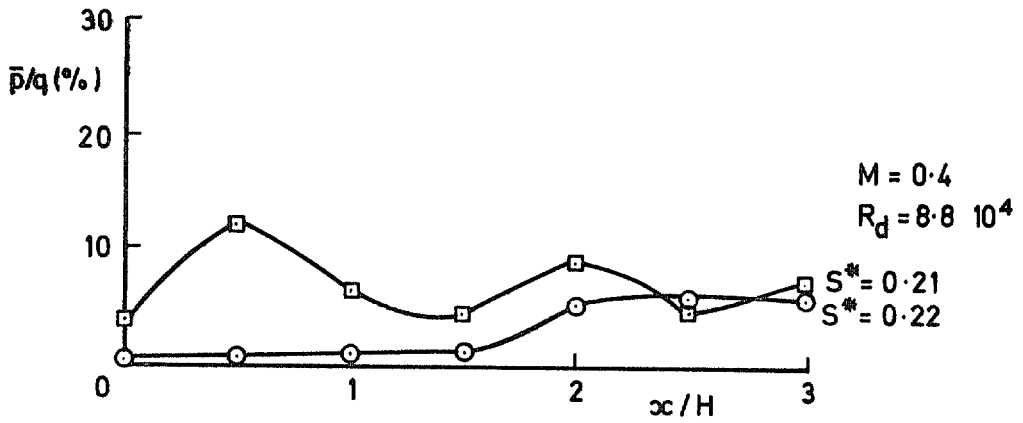
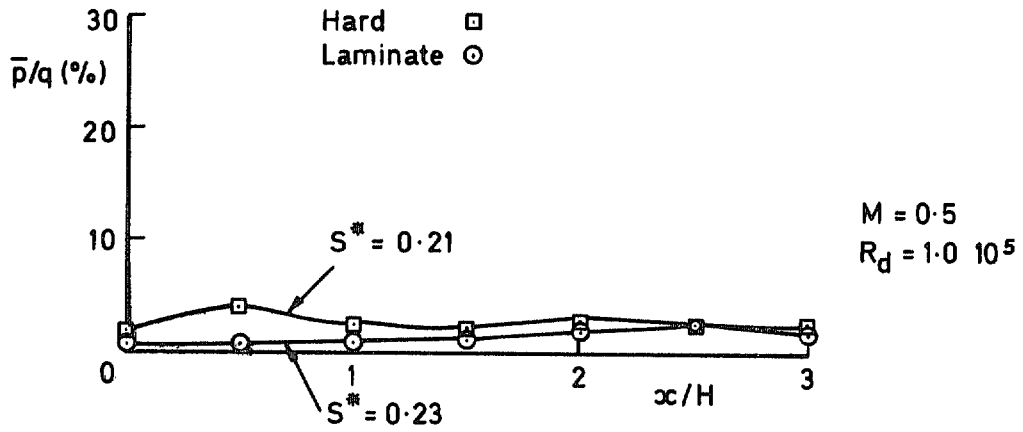


Fig 8 contd

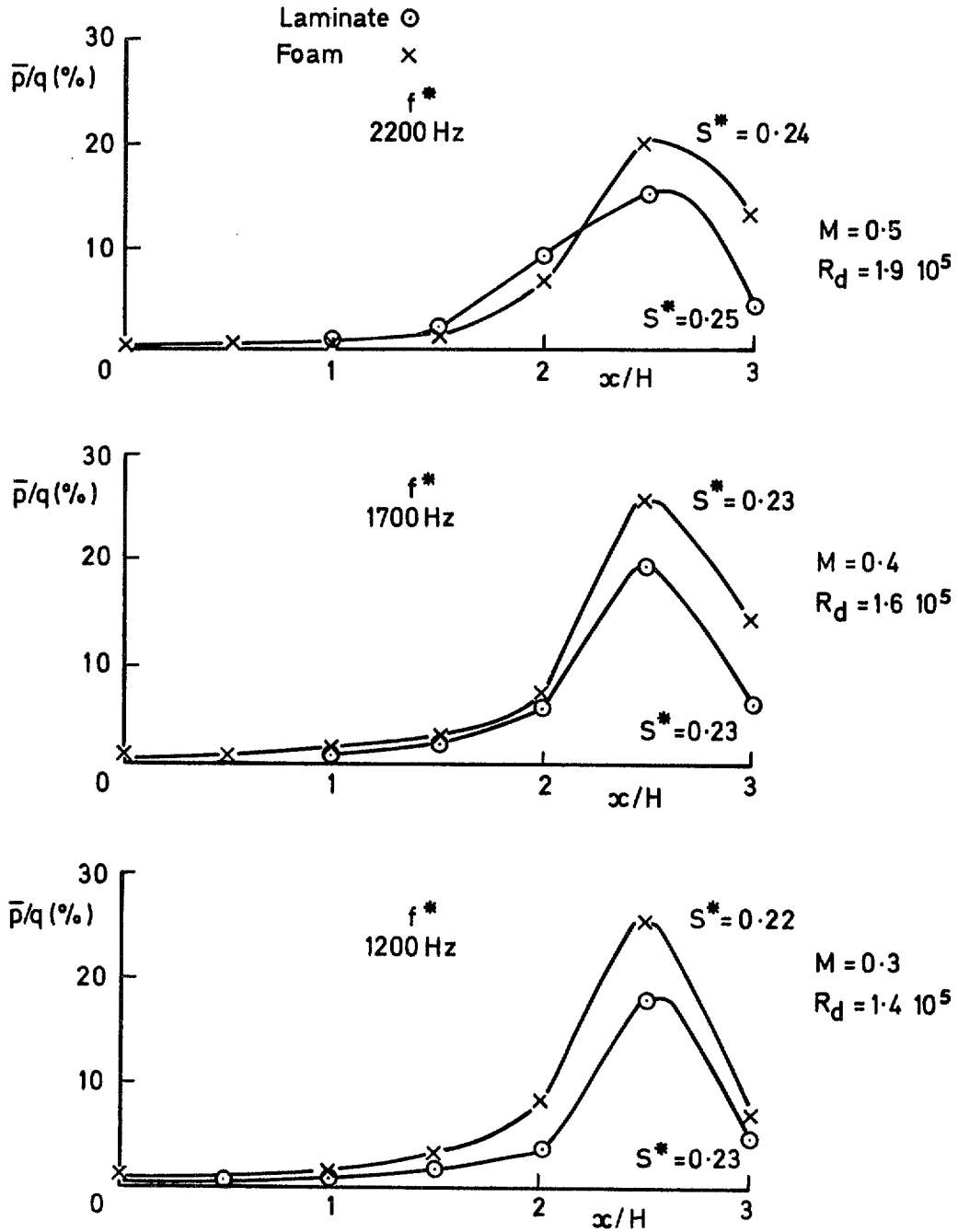


Fig 9 Side wall pressure fluctuations in closed working sections with alternative wall materials  $d = 18$  mm

Fig 10

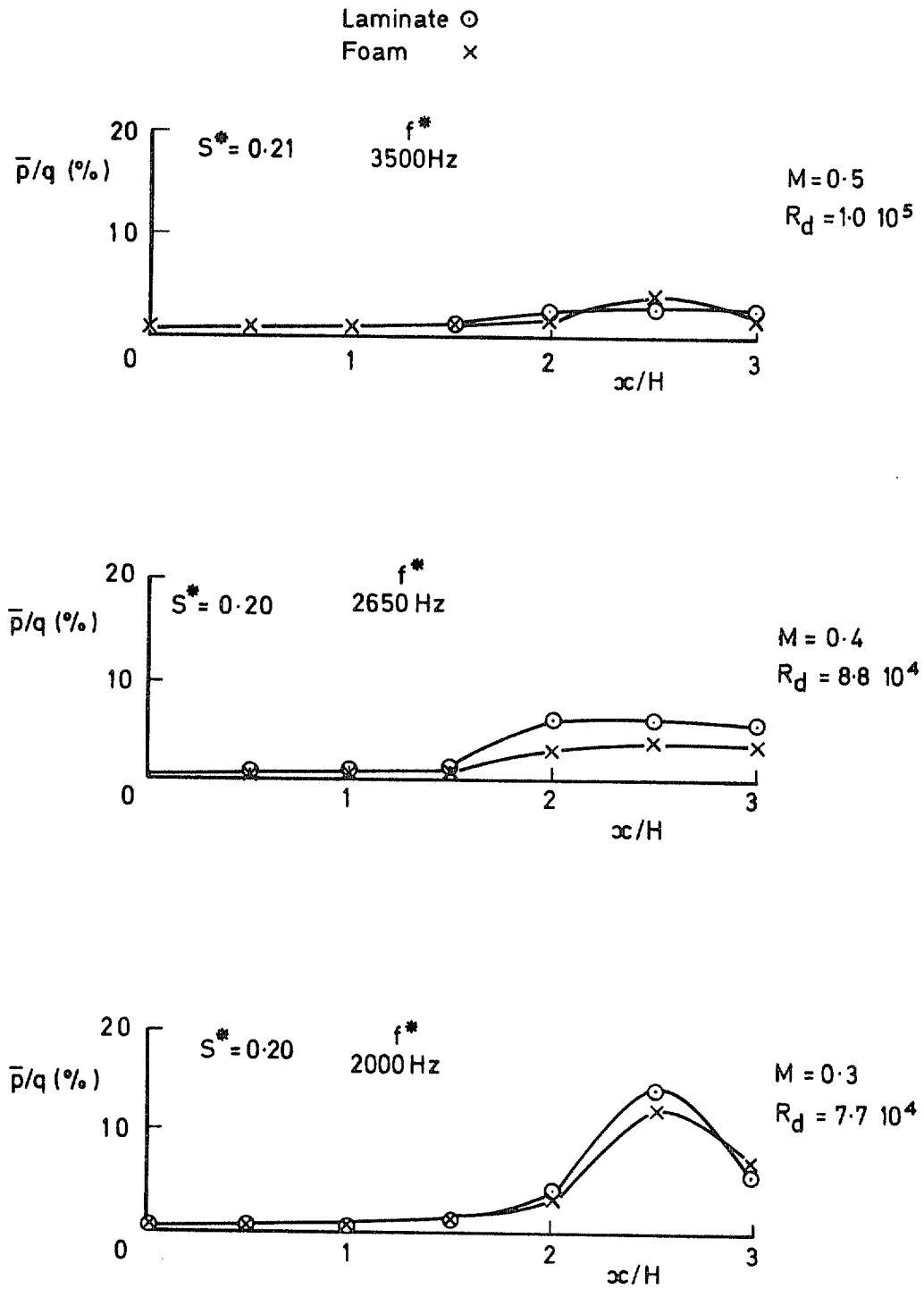


Fig 10 Side wall pressure fluctuations in closed working sections with alternative wall materials  $d = 10 \text{ mm}$

Fig 11

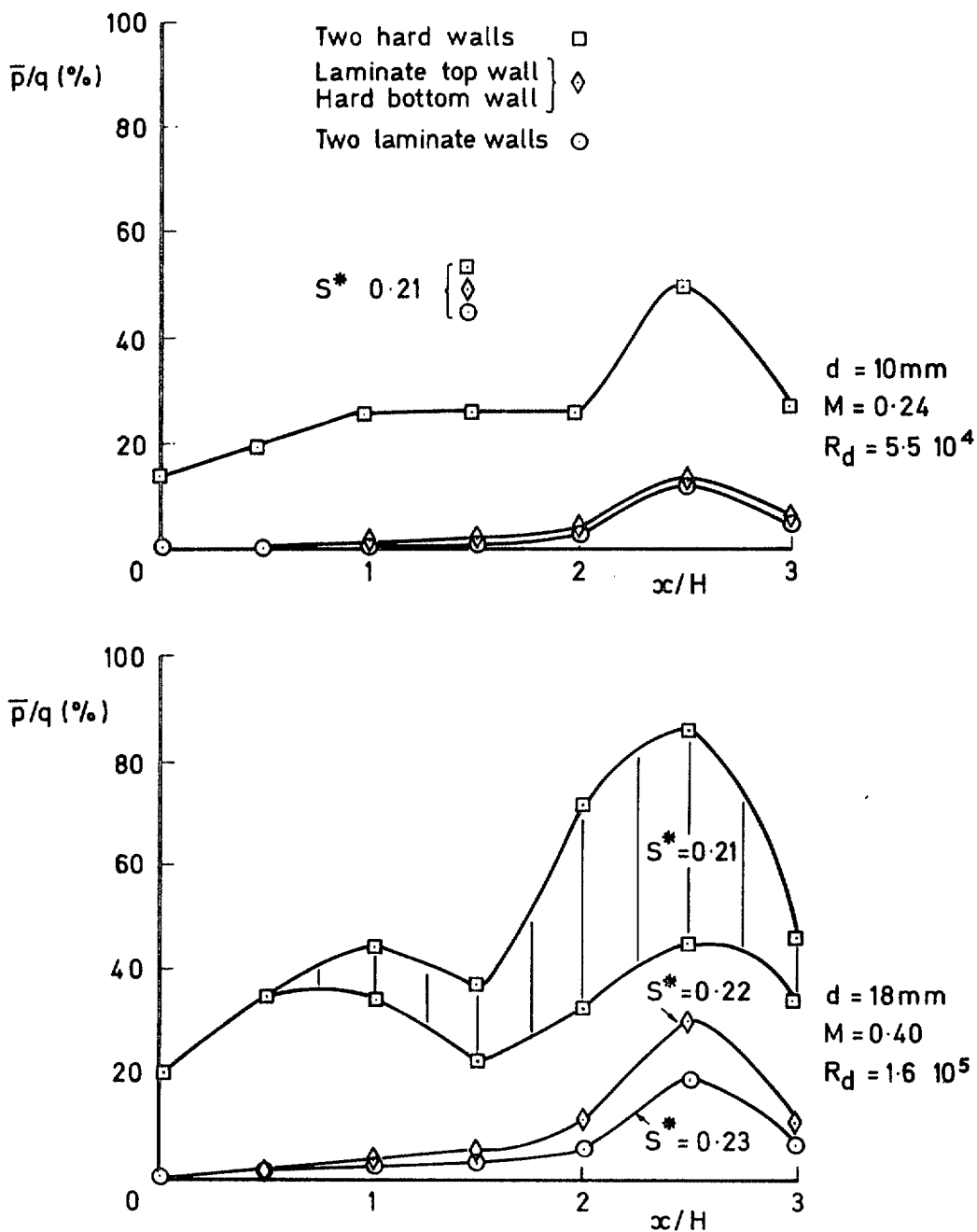


Fig 11 4in x 4in tunnel — closed working sections — comparison of symmetric and asymmetric wall configurations

Fig 12

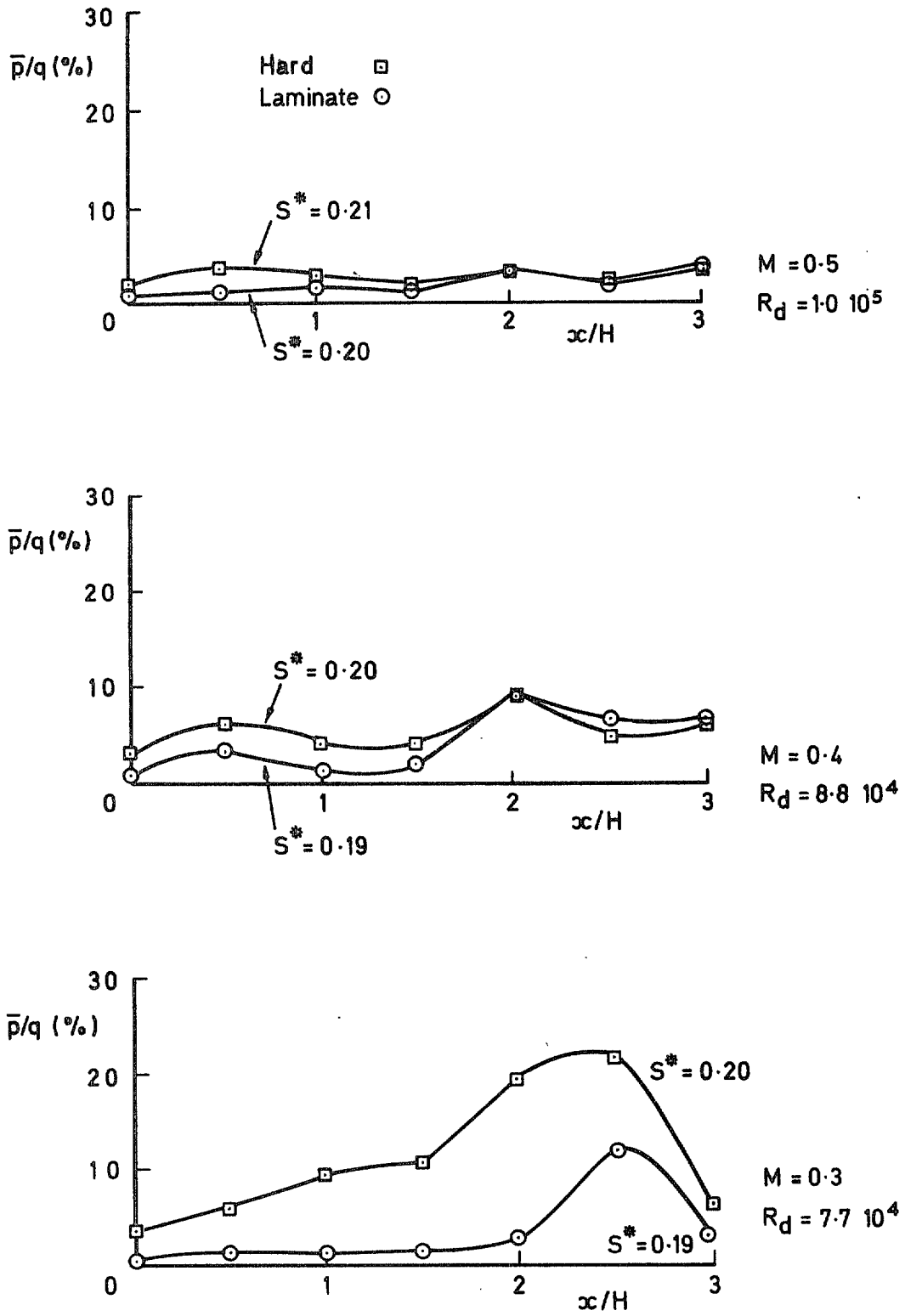
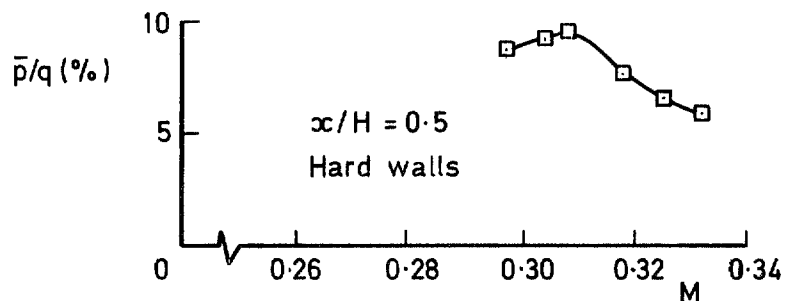
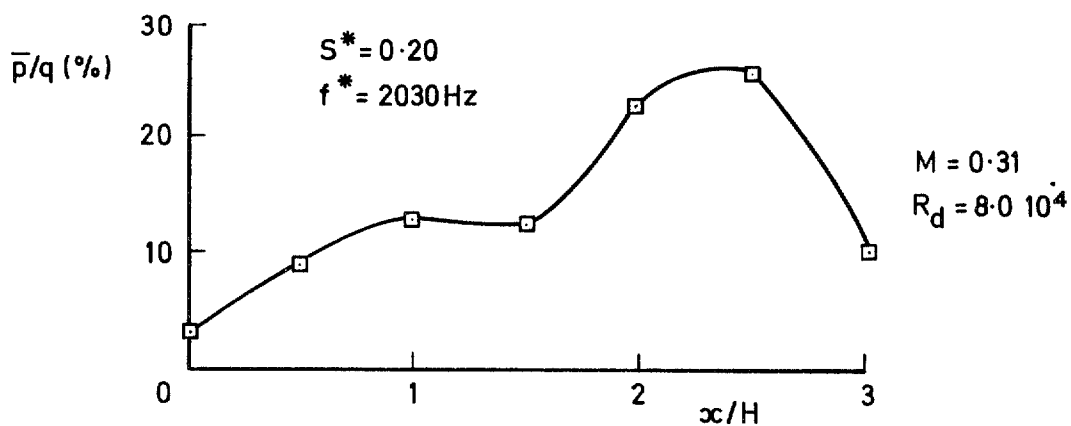


Fig 12 Interference in slotted working sections:  $d = 10$  mm, two wall materials

**Fig 13a&b**



a Broad-band pressure fluctuations near resonance condition



b Narrow-band pressure fluctuations at resonance condition  $d = 10 \text{ mm}$

**Fig 13a&b Resonance in slotted working sections  $d = 10 \text{ mm}$**

Fig 14

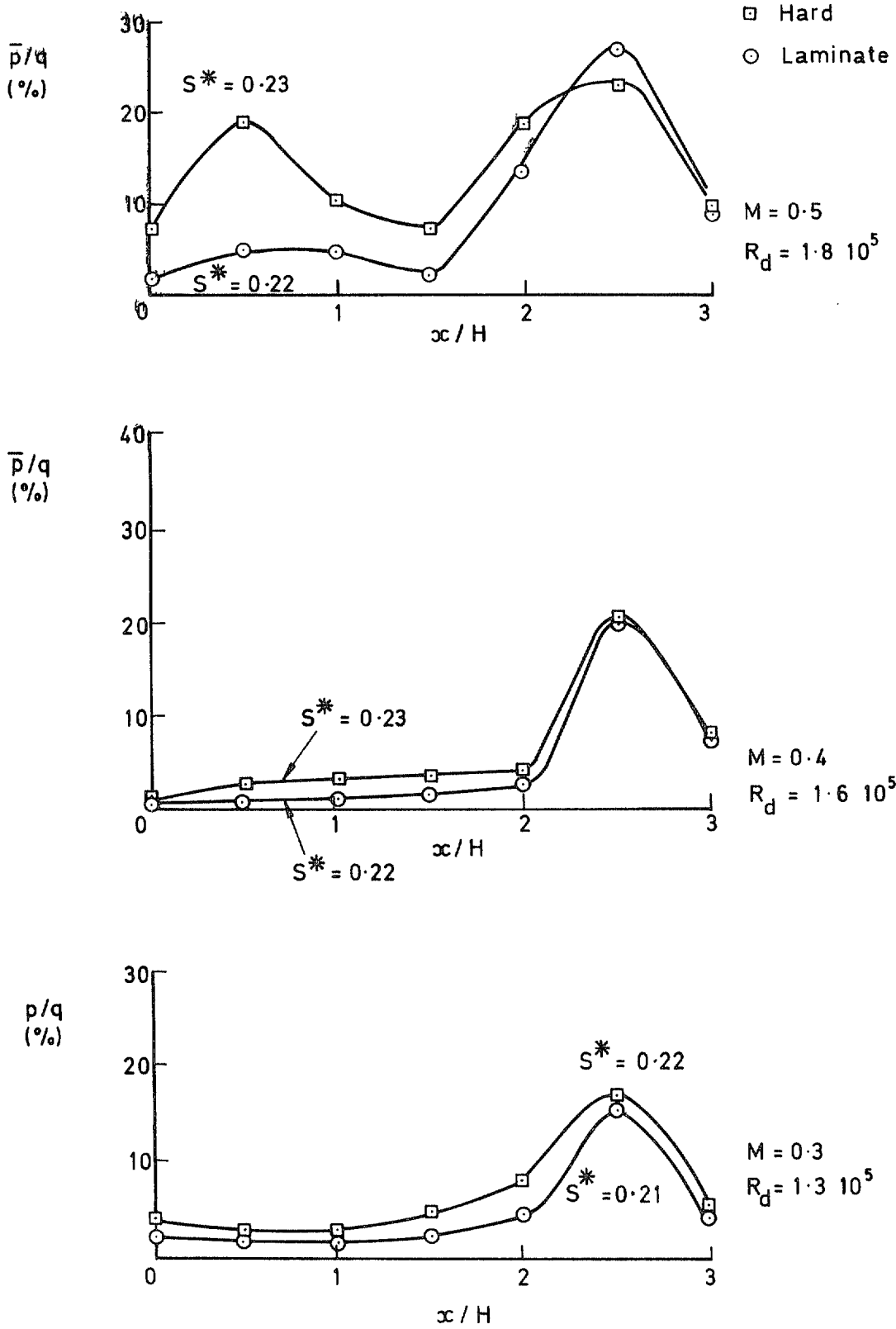
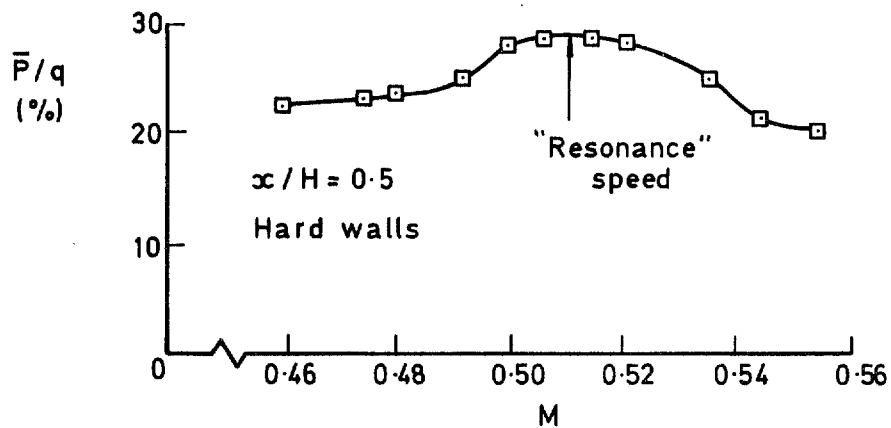


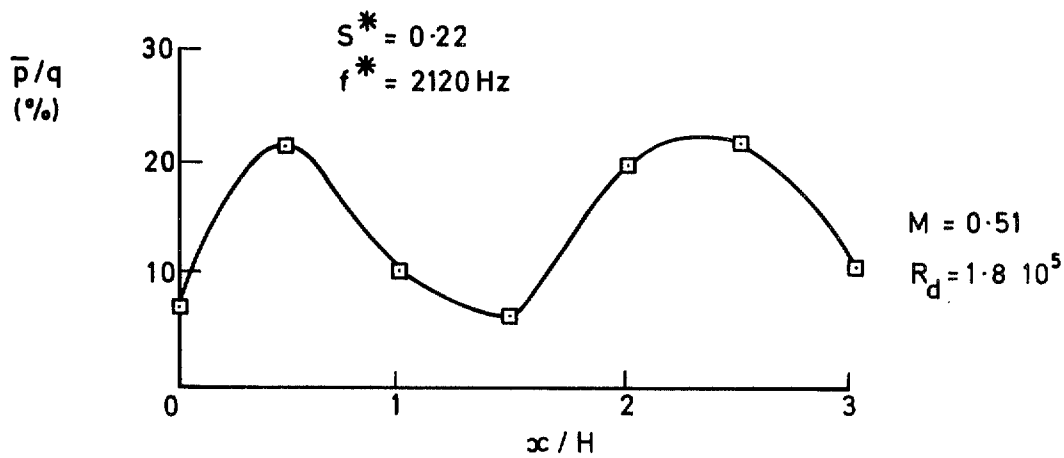
Fig 14 Interference in slotted working sections:  $d = 18$  mm, two wall materials



Fig 15a&b



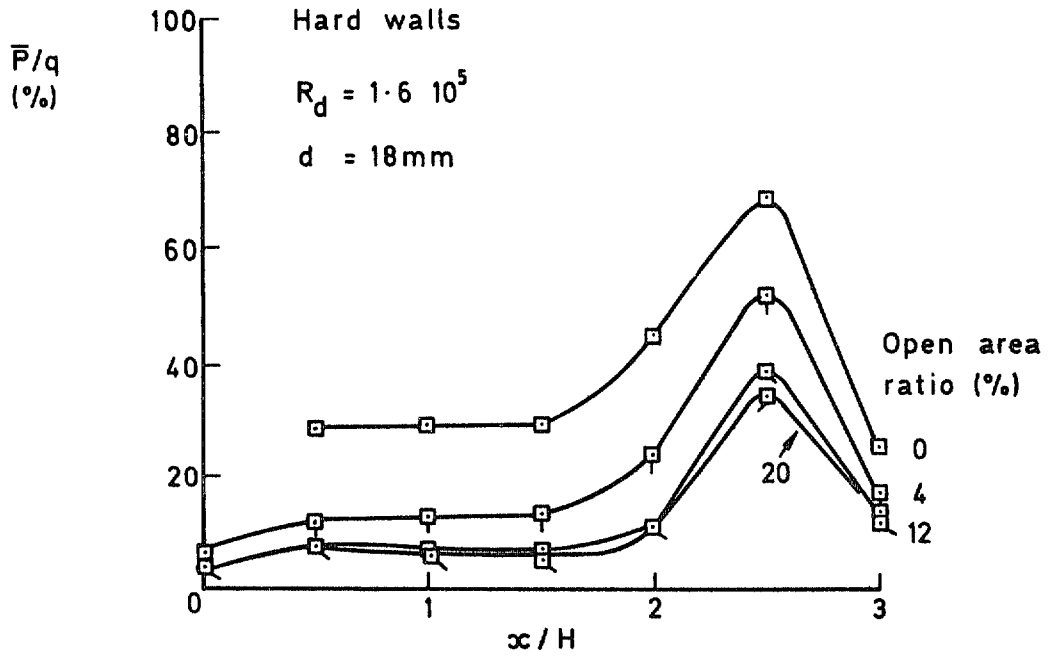
a Broad-band pressure fluctuations near "resonance" condition



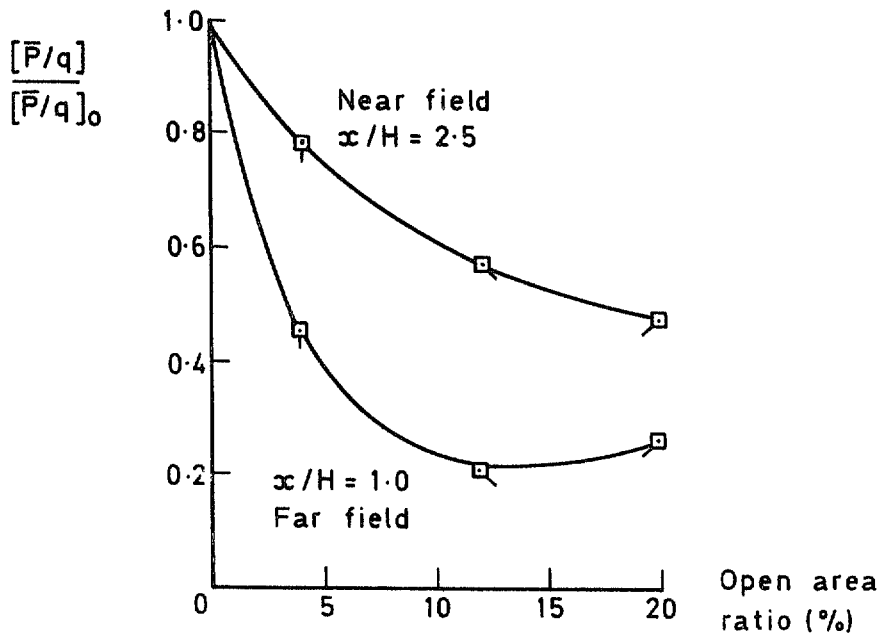
b Narrow-band pressure fluctuations at "resonance" condition

Fig 15a&b Possible resonance in slotted working section  $d = 18$  mm

Fig 16a&b



a Broad band pressure fluctuations



b Attenuation of pressure fluctuations with open area ratio

Fig 16a&b Influence of open area ratio on resonant pressure fluctuations slotted working section  $M = 0.4$

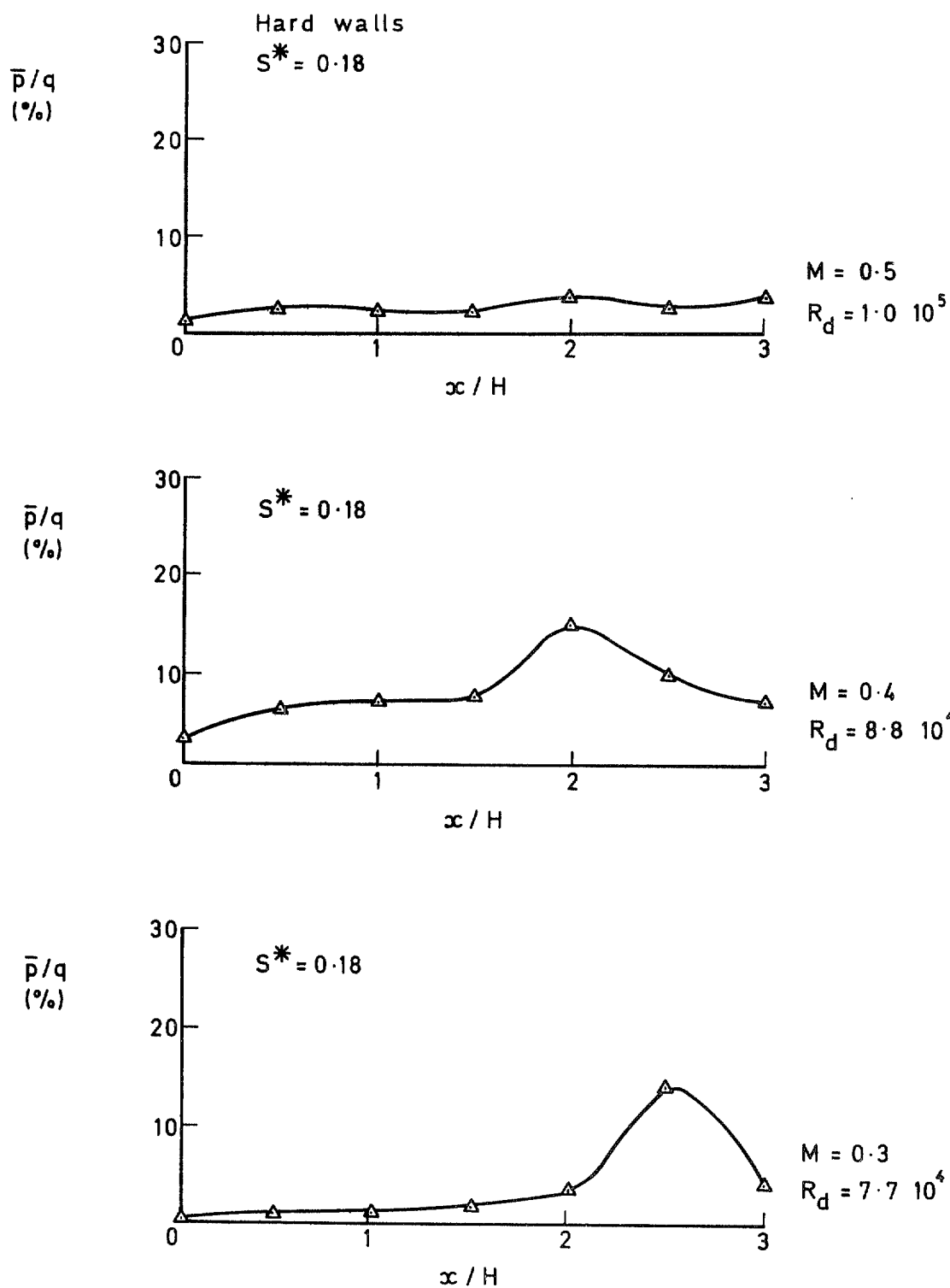


Fig 17 Side wall pressure fluctuations in perforated working section  $d = 10$  mm

Fig 18

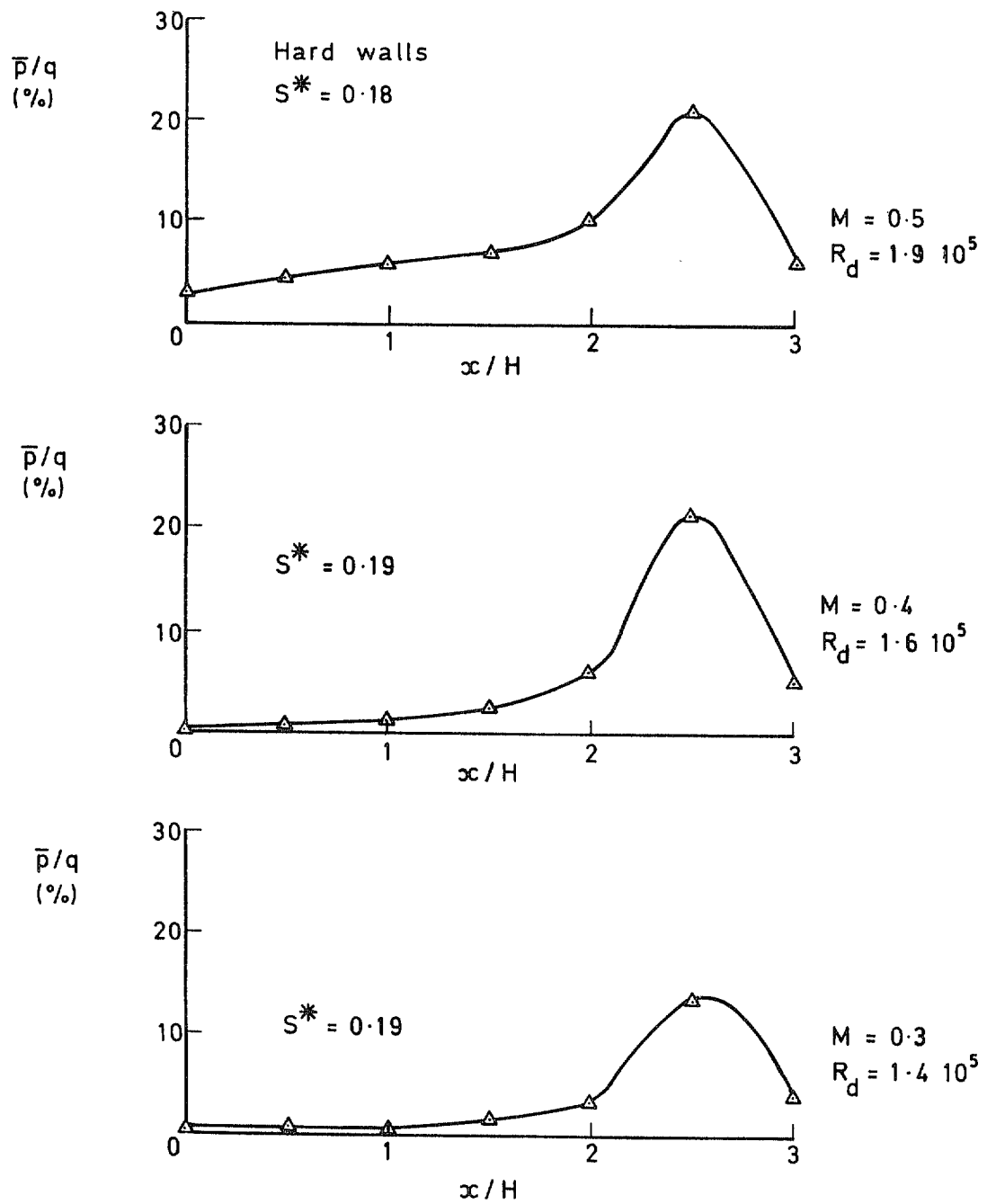
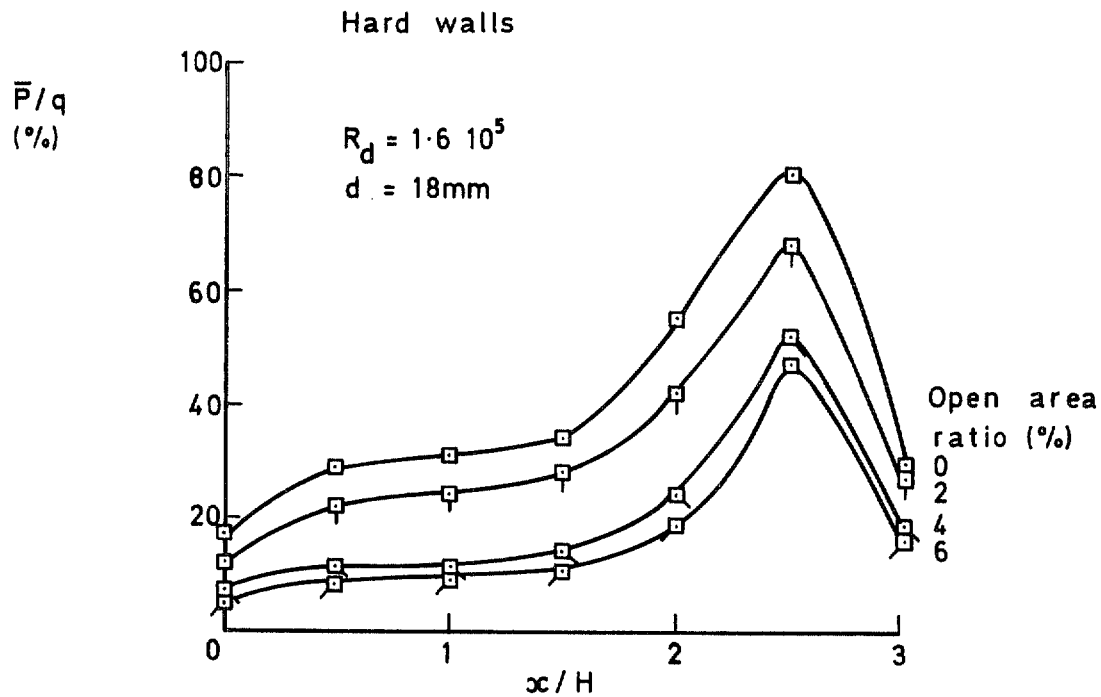
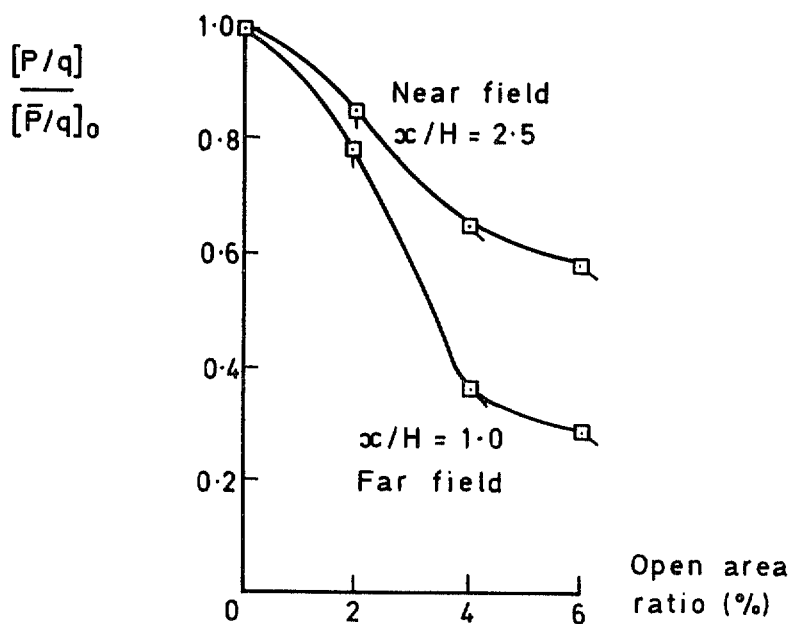


Fig 18 Side wall pressure fluctuations in perforated working section  $d = 18$  mm

Fig 19a&b



a Broad band pressure fluctuations



b Attenuation of pressure fluctuations

Fig 19a&b Influence of open area ratio on pressure fluctuations and resonance-perforated working section  $M = 0.4$

Fig 20

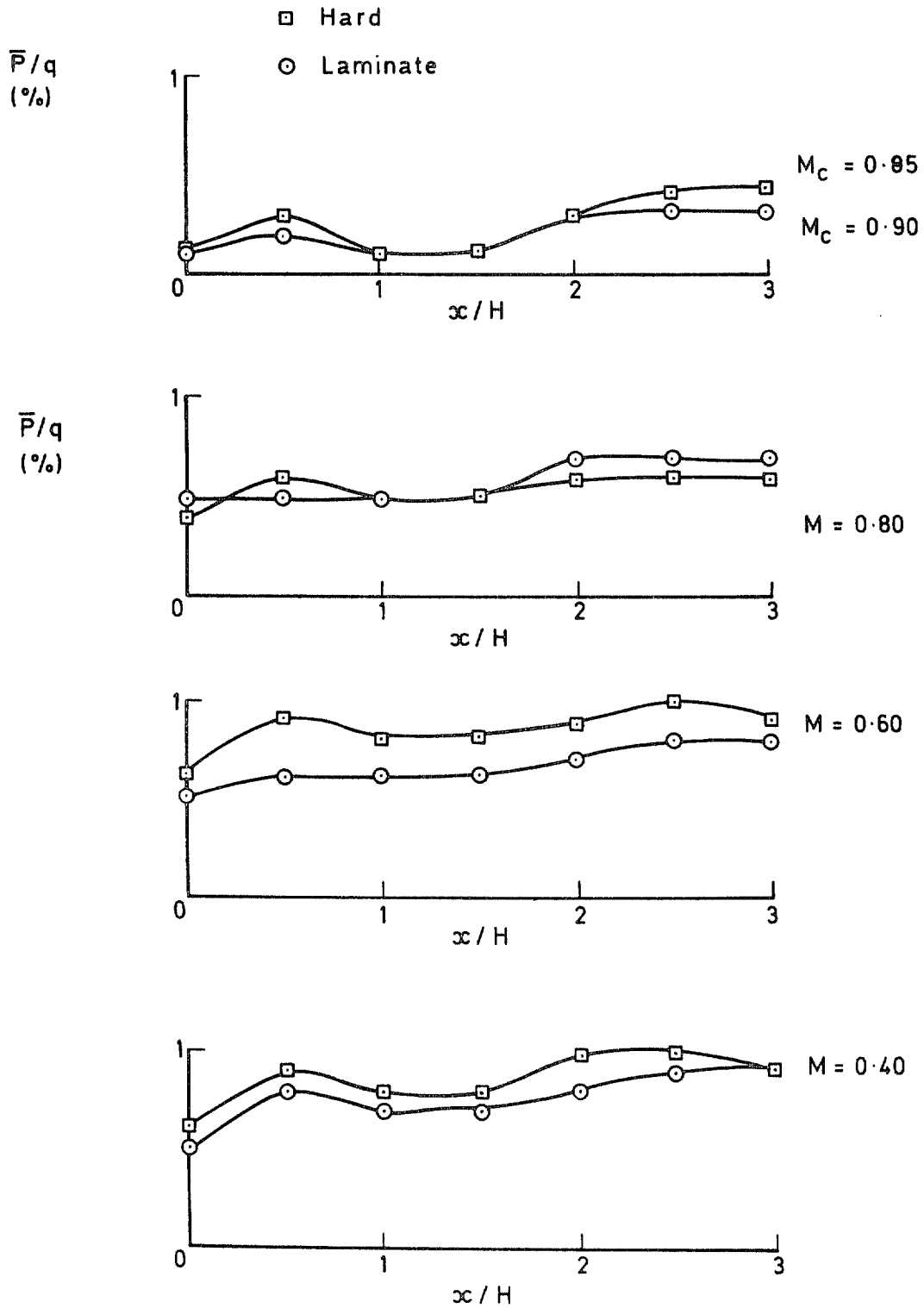


Fig 20 4in x 4in closed working sections — variation of broadband pressure fluctuations along empty tunnel

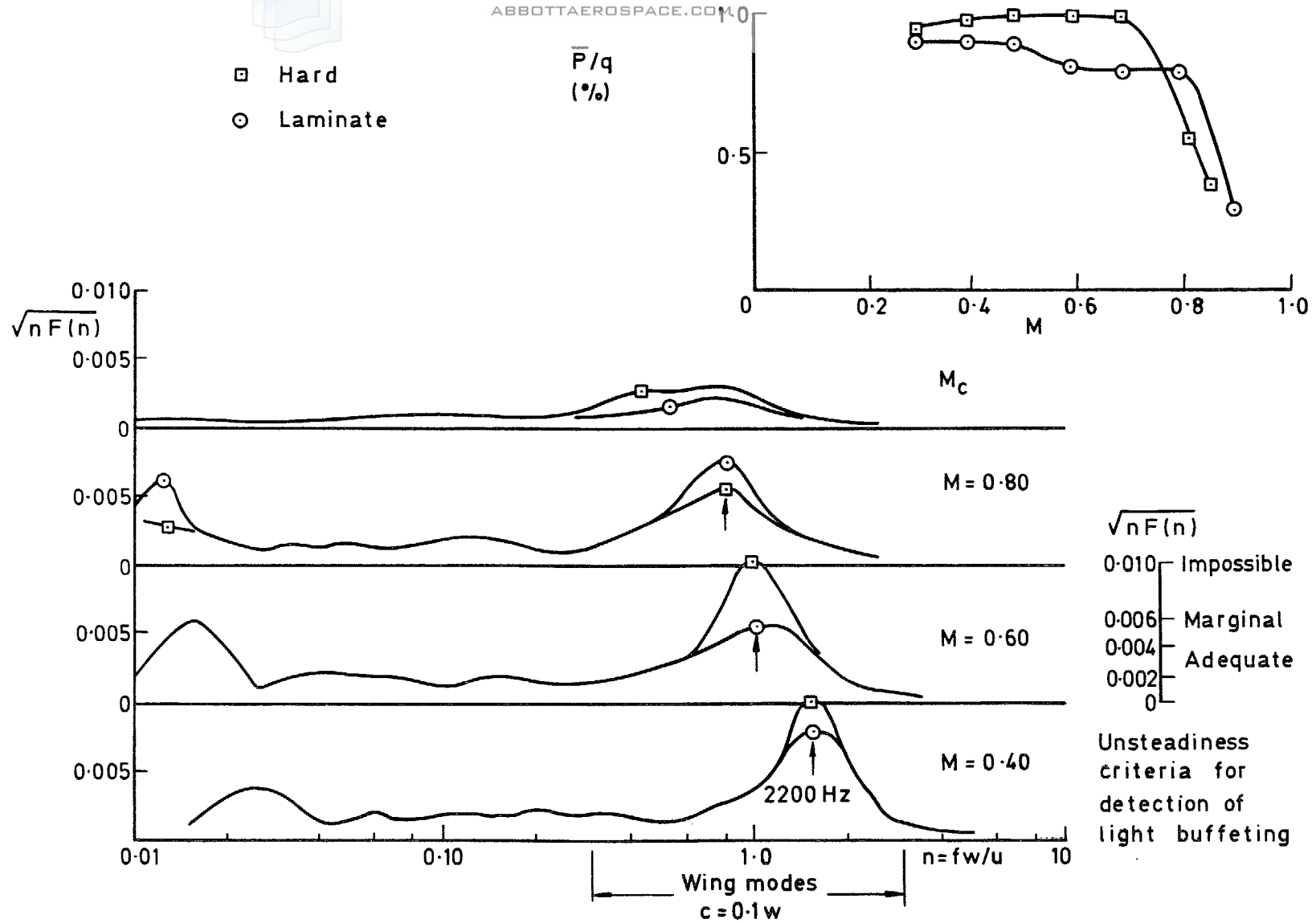


Fig 21 4in x 4in closed working sections – pressure fluctuation at  $x/H = 2.5$  tunnel empty

Fig 22

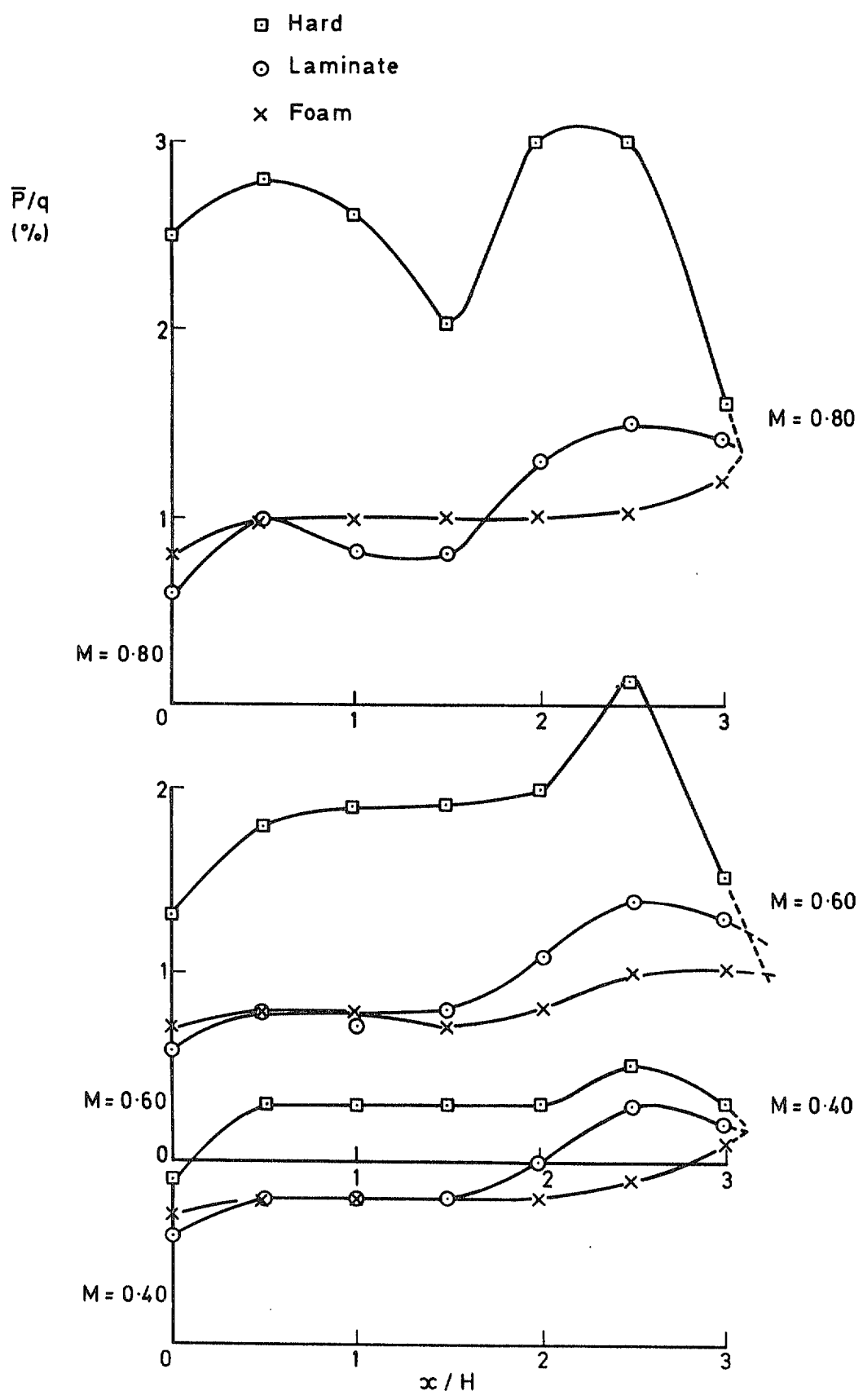


Fig 22 4in x 4in slotted working sections — variation of broadband pressure fluctuations along tunnel (empty)



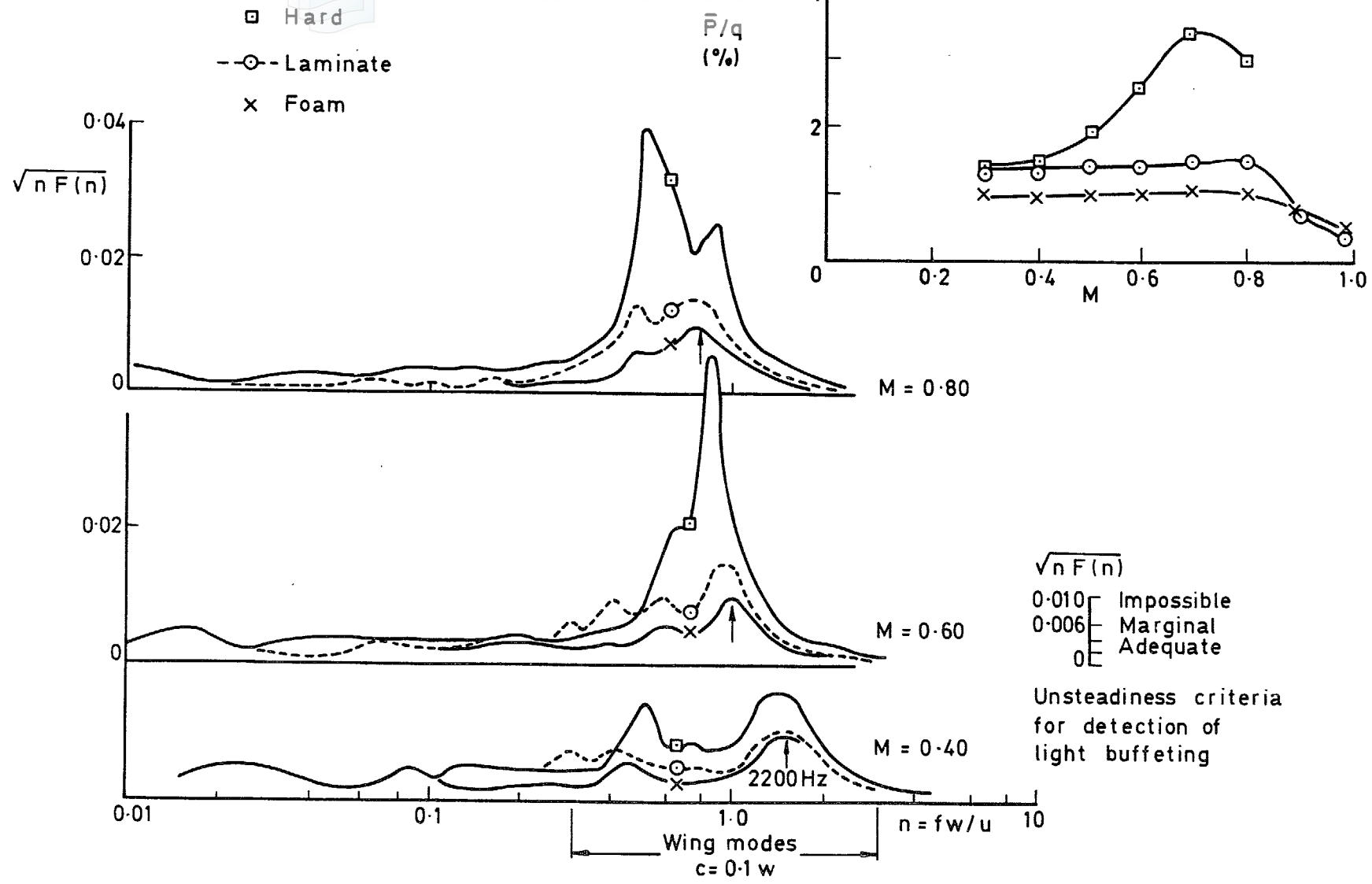


Fig 23 4in x 4in slotted working sections – pressure fluctuations at X/H = 2.5 tunnel empty

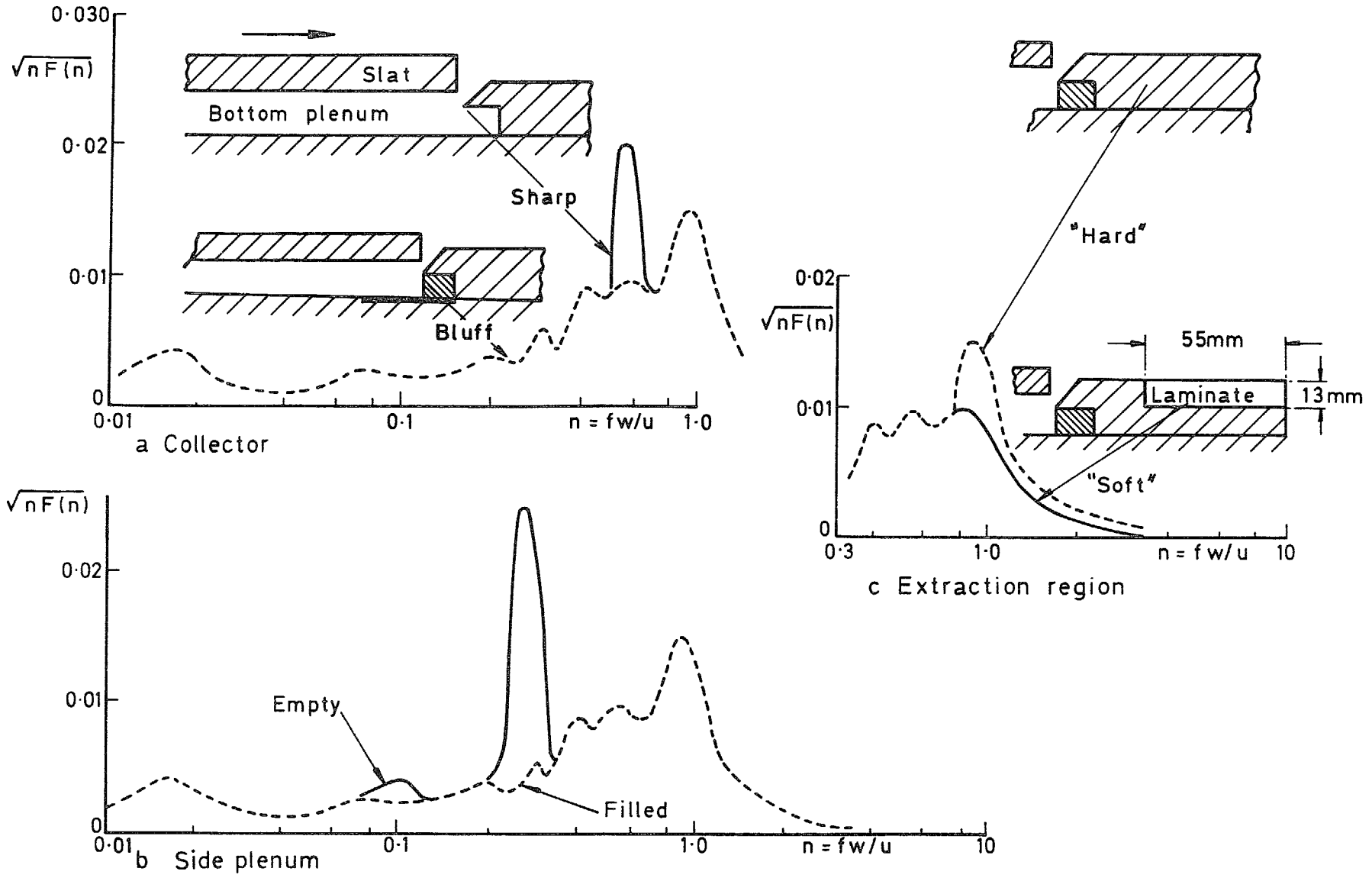


Fig 24a-c

Fig 24a-c 4in x 4in laminate slotted working section – modifications to reduce pressure fluctuations – tunnel empty –  $x/H = 2.5$   $M = 0.60$

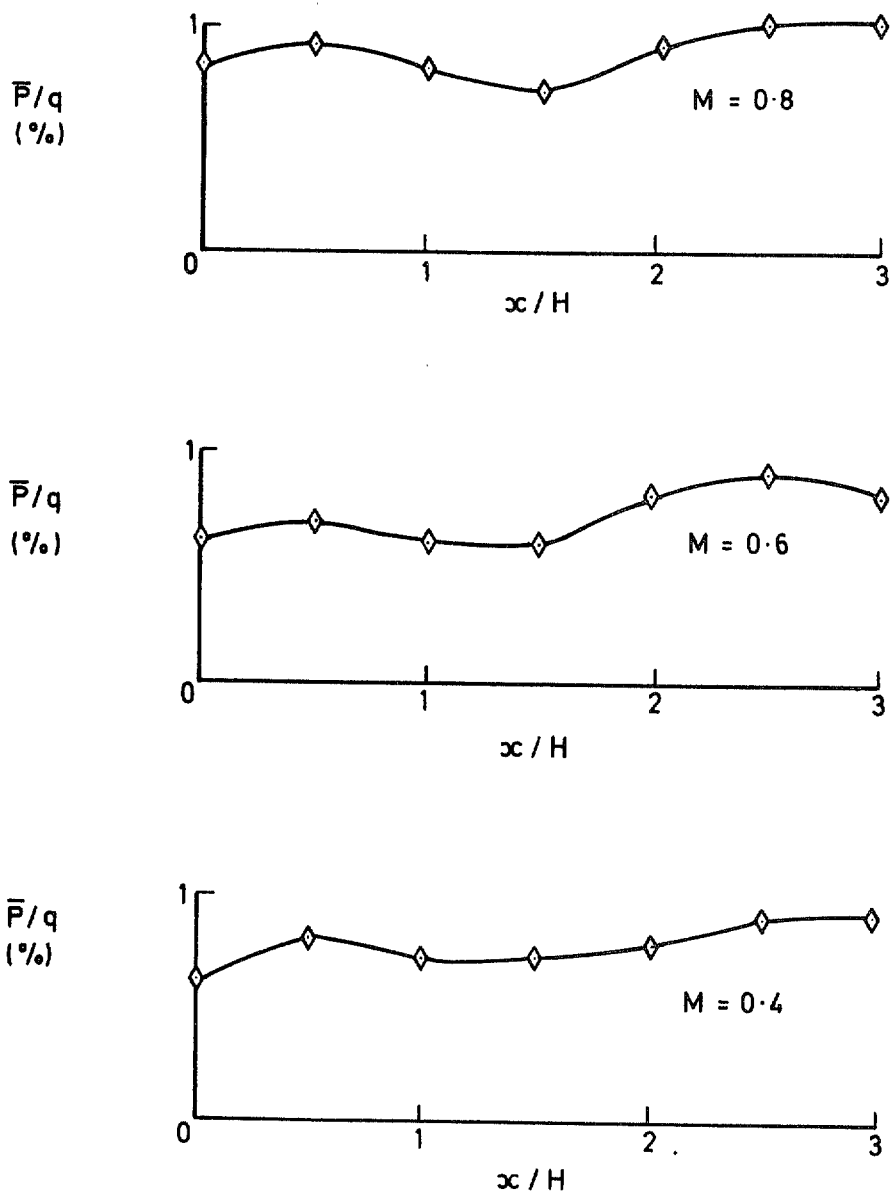


Fig 25 4in x 4in perforated working section — variation of broadband pressure fluctuations along empty tunnel

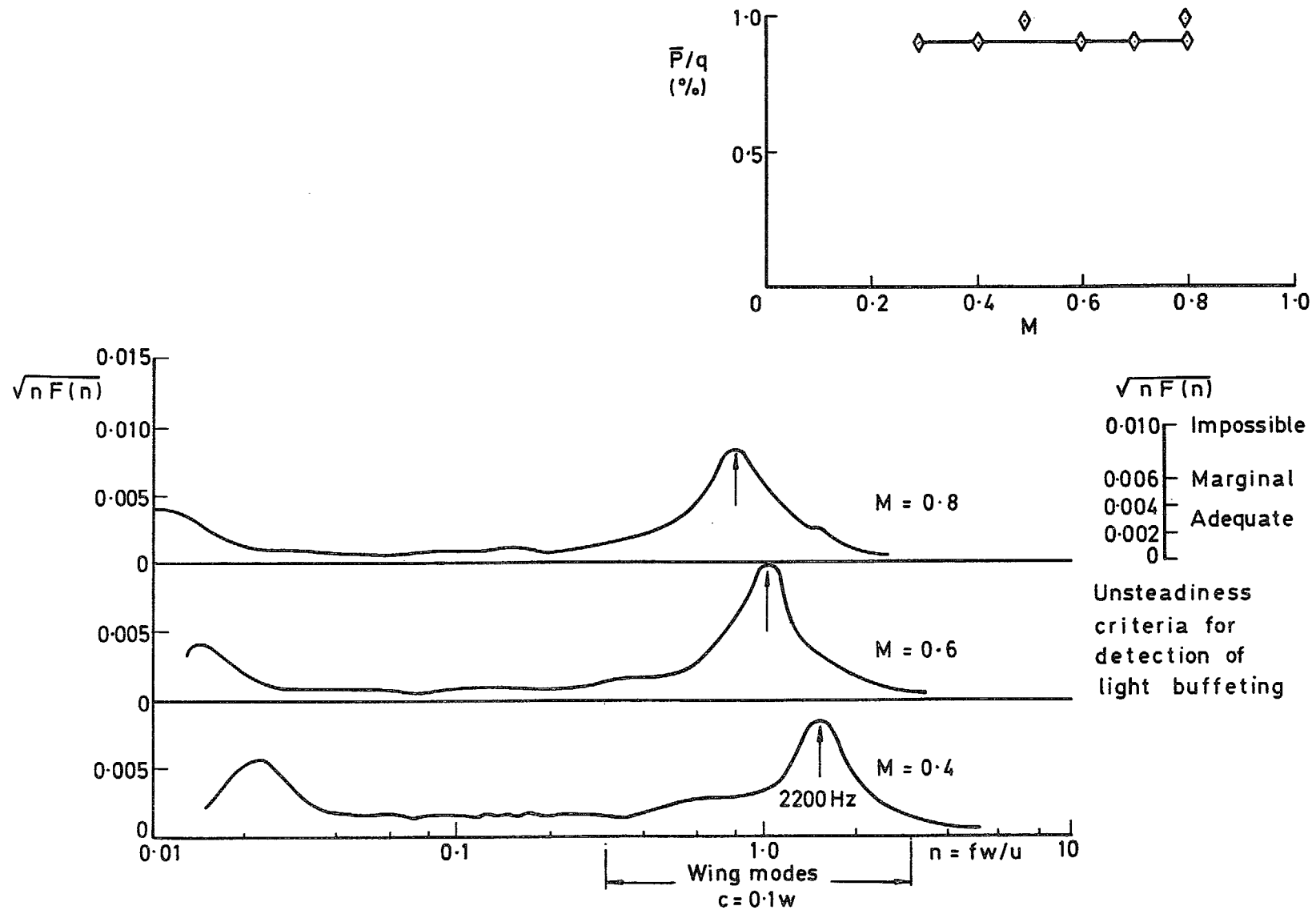


Fig 26 4in x 4in perforated working section – pressure fluctuations at  $x/H = 2.5$  tunnel empty

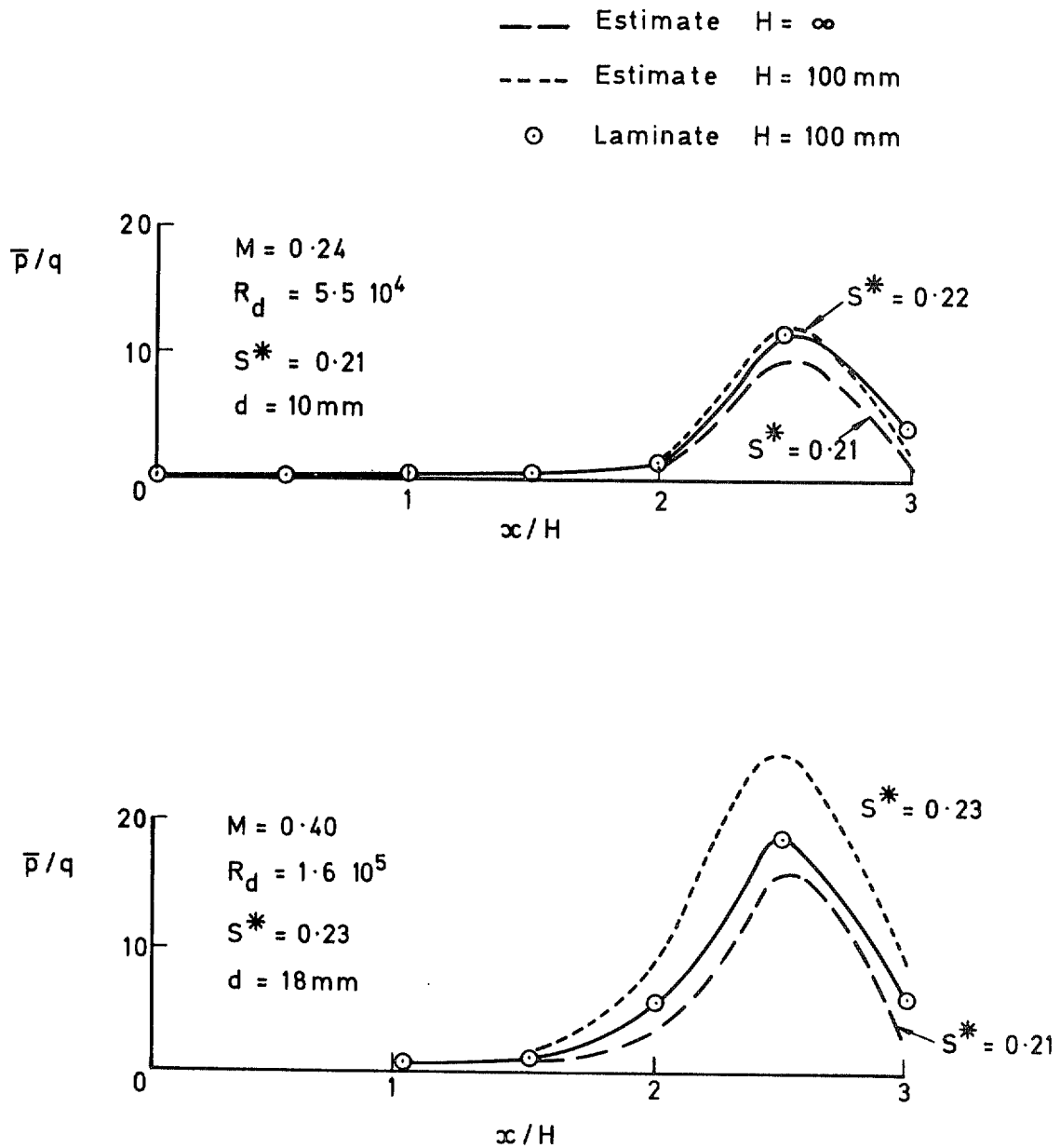
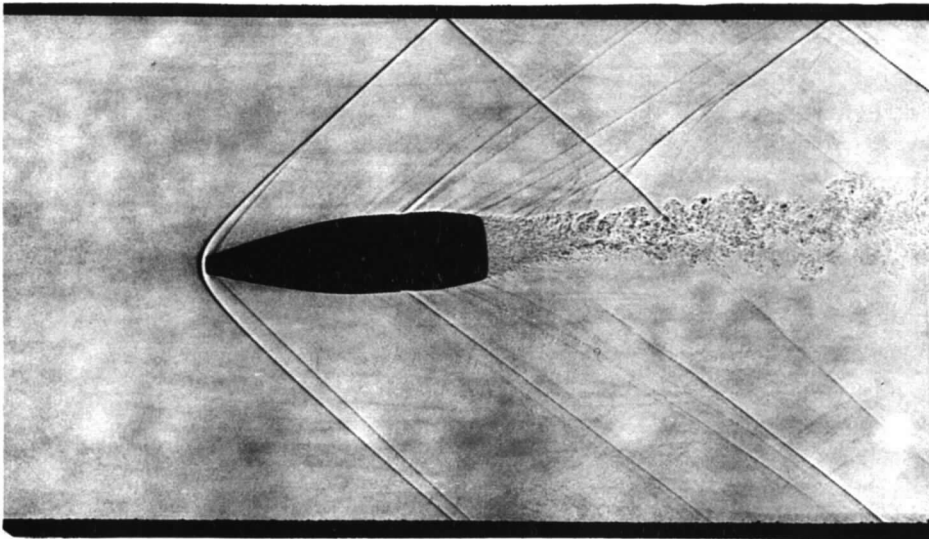


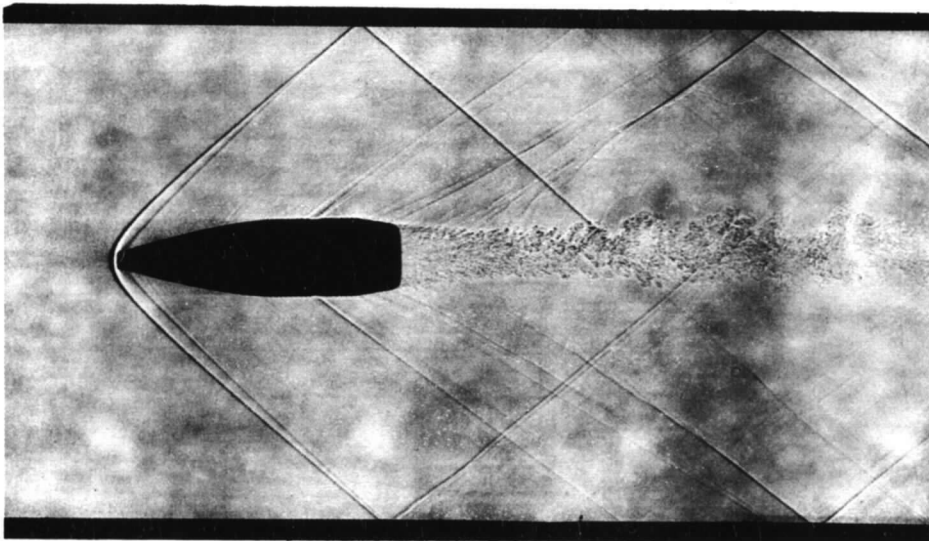
Fig 27 Estimated interference free pressure fluctuations in closed working section

Fig 28a-c



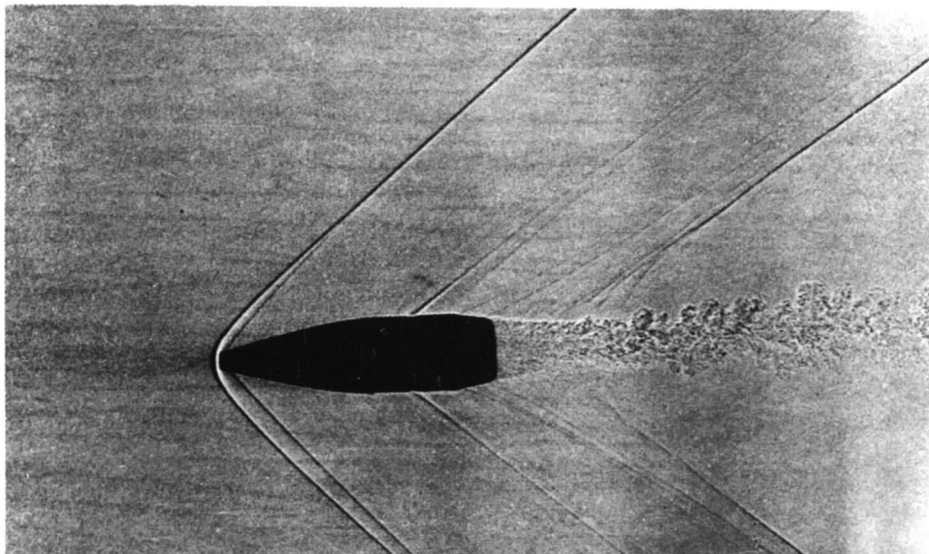
Hard

a. Foam



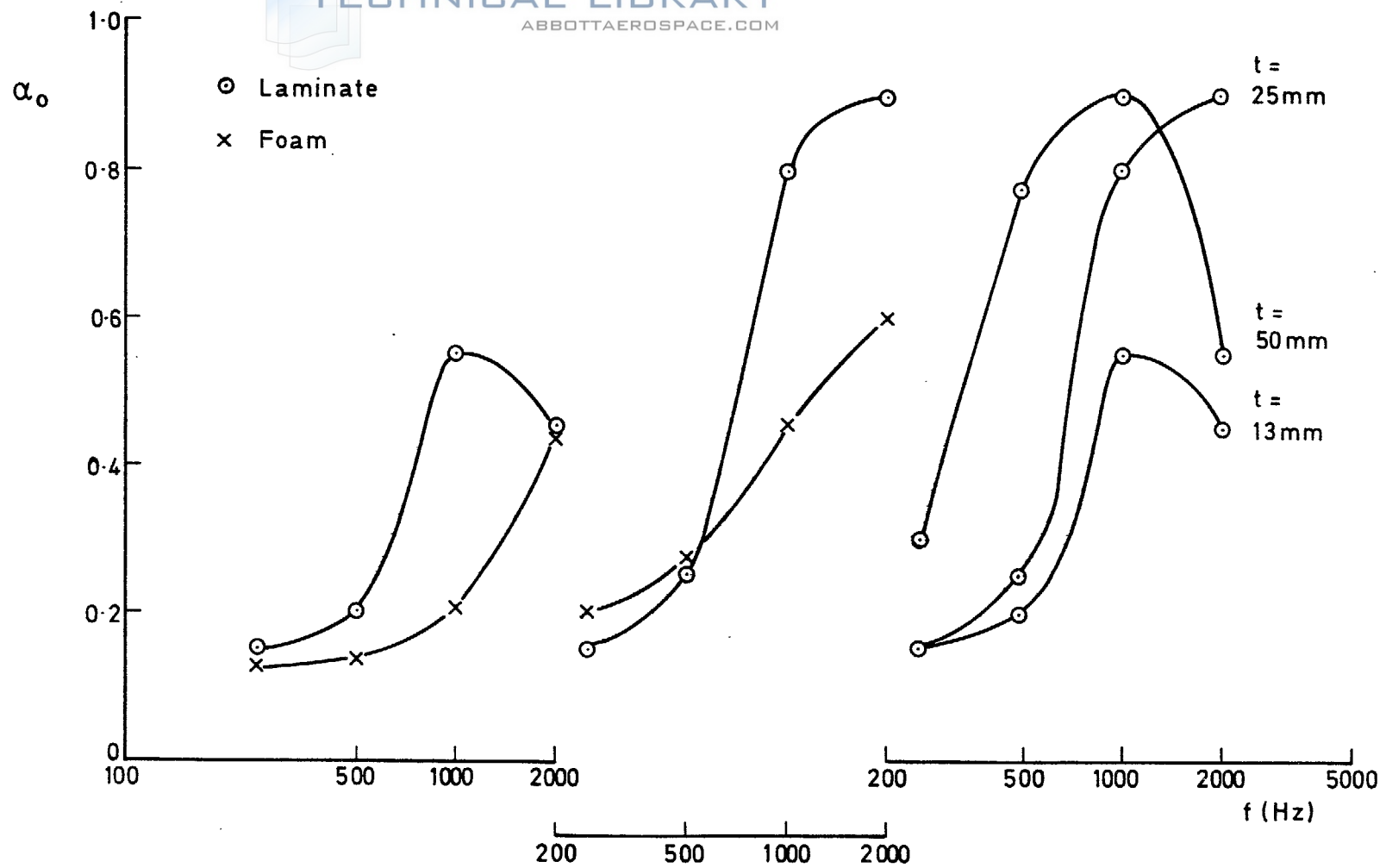
Hard

b. Laminate



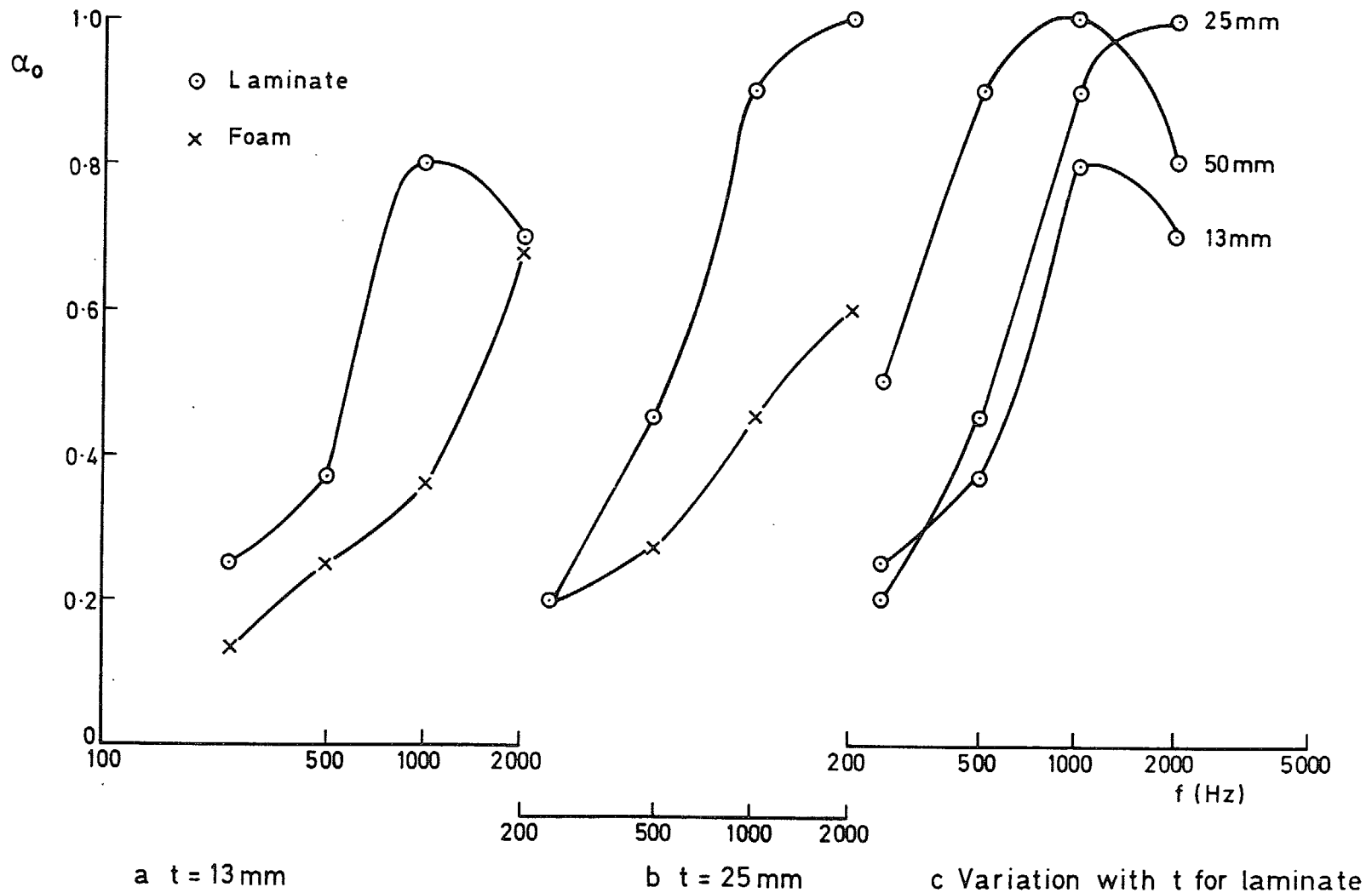
c. Free air

Fig 28a-c Reflected shock waves at  $M = 1.7$



a  $t = 13\text{ mm}$                       b  $t = 25\text{ mm}$                       c Variation with  $t$  for laminate

Fig 29a-c Normal incidence sound absorption coefficients for wall materials



Printed in England for Her Majesty's Stationery Office by the Royal Aircraft Establishment, Farnborough, Hants. Dd. 586386 K4 11/76.

Fig 30a-c Random incidence sound absorption coefficients for wall materials



© *Crown copyright*

1979

Published by  
HER MAJESTY'S STATIONERY OFFICE

*Government Bookshops*

49 High Holborn, London WC1V 6HB  
13a Castle Street, Edinburgh EH2 3AR  
41 The Hayes, Cardiff CF1 1JW  
Brazennose Street, Manchester M60 8AS  
Southey House, Wine Street, Bristol BS1 2BQ  
258 Broad Street, Birmingham B1 2HE  
80 Chichester Street, Belfast BT1 4JY

*Government Publications are also available  
through booksellers*

R & M No.3831  
ISBN 0114 71164